

Washington University in St. Louis
Washington University Open Scholarship

All Theses and Dissertations (ETDs)

January 2010

Modeling Aerial Refueling Operations

Allen McCoy

Washington University in St. Louis

Follow this and additional works at: <https://openscholarship.wustl.edu/etd>

Recommended Citation

McCoy, Allen, "Modeling Aerial Refueling Operations" (2010). *All Theses and Dissertations (ETDs)*. 235.
<https://openscholarship.wustl.edu/etd/235>

This Dissertation is brought to you for free and open access by Washington University Open Scholarship. It has been accepted for inclusion in All Theses and Dissertations (ETDs) by an authorized administrator of Washington University Open Scholarship. For more information, please contact digital@wumail.wustl.edu.

WASHINGTON UNIVERSITY IN ST. LOUIS
School of Engineering and Applied Science
Department of Electrical and Systems Engineering

Thesis Examination Committee:
Ervin Rodin, Co-Chair
Heinz Schaettler, Co-Chair
Norman Katz
Hiro Mukai
David Peters

MODELING AERIAL REFUELING OPERATIONS

by

Allen B. McCoy III

A dissertation presented to the School of Engineering
of Washington University in partial fulfillment of the
requirements for the degree of

DOCTOR OF SCIENCE

May 2010
Saint Louis, Missouri

copyright by
Allen B. McCoy III
2010

ABSTRACT OF THE THESIS

Modeling Aerial Refueling Operations

by

Allen B. McCoy III

Doctor of Science in Systems Science and Mathematics

Washington University in St. Louis, 2010

Research Advisor: Professor Ervin Y. Rodin

Aerial Refueling (AR) is the act of offloading fuel from one aircraft (the tanker) to another aircraft (the receiver) in mid flight. Meetings between tanker and receiver aircraft are referred to as AR events and are scheduled to: escort one or more receivers across a large body of water; refuel one or more receivers; or train receiver pilots, tanker pilots, and boom operators. In order to efficiently execute the Aerial Refueling Mission, the Air Mobility Command (AMC) of the United States Air Force (USAF) depends on computer models to help it make tanker basing decisions, plan tanker sorties, schedule aircraft, develop new organizational doctrines, and influence policy. We have worked on three projects that have helped AMC improve its modeling and decision making capabilities.

Optimal Flight Planning: Currently Air Mobility simulation and optimization software packages depend on algorithms which iterate over three dimensional fuel flow tables to compute aircraft fuel consumption under changing flight conditions. When a high degree of fidelity is required, these algorithms use a large amount of

memory and CPU time. We have modeled the rate of aircraft fuel consumption with respect to AC Gross Weight, Altitude and Airspeed. When implemented, this formula will decrease the amount of memory and CPU time needed to compute sortie fuel costs and cargo capacity values. We have also shown how this formula can be used in optimal control problems to find minimum costs flight plans.

Tanker Basing Demand Mismatch Index: Since 1992, AMC has relied on a Tanker Basing/AR Demand Mismatch Index which aggregates tanker capacity and AR demand data into six regions. This index was criticized because there were large gradients along regional boundaries. Meanwhile tankers frequently cross regional boundaries to satisfy the demand for AR support. In response we developed continuous functions to score locations with respect to their proximity to demand for AR support as well as their isolation from existing tanker bases.

Optimal Scheduling Because most of the tanker resources are controlled by individual Air National Guard Units there is little to no central authority coordinating tanker and receiver training schedules. We have been able to show that significant flying hour savings could be achieved if National Guard tanker units were to yield some of their scheduling autonomy to a central authority which was charged with the responsibility of matching tanker training requirements to receiver training requirements.

Acknowledgments

This work would not have been possible without the assistance of Dave Merrill and his team in the Air Mobility Command's Directorate of Analysis Assessments and Lessons Learned (AMC A9) who poured out significant moral, technical, material, and advisory support as well as heaps of encouragement. Special thanks are owed to Pete Szabo, Eugene Miller, LtCol. Brian Lloyd, Jim Donovan, John O'Neil, Ron McGarvey, Chris Jones, Jan Howard, and Mike Metzger. This work was also significantly shaped by Airmen, civilians, and contractors at HQ AMC outside of AMC A9. Special thanks are also owed to Brad Davis, LtCol. Lee Erickson, Maj. Steve Hendren, Lee Winter, Dan Derrick, and Tina Wallace.

Allen B. McCoy III

Washington University in Saint Louis
May 2010

Dedicated to my Parents.

The best gift parents can give their kids is an education. Thanks for all of the encouragement and support. You guys really went the extra mile.

Contents

Abstract	ii
Acknowledgments	iv
List of Figures	viii
1 Optimal Control Formulations of Tanker Sortie Planning Problems	1
1.1 Introduction	1
1.2 The Basic Mechanics of Powered Flight	3
1.3 The Rate of Fuel Consumption	12
1.4 Further Notation	16
1.5 Estimators For Unknown Coefficients	17
1.6 Estimation Results	21
1.7 An Optimal Control Formulation of the Tanker Sortie Fuel Planning Problem	26
1.7.1 Final Cruise Segment	28
1.7.2 AR Segment	29
1.7.3 Inter AR Cruise Segment	30
1.7.4 Initial Cruise Segment	30
1.7.5 Initial Climb Segment	31
1.7.6 Example Implementation	32
1.8 Suggestions for Future Research	33
2 Tanker Basing Demand Mismatch Index	34
2.1 Introduction	34
2.2 The Ideal TBDMI	37
2.3 Constructing New Supply and Demand Scores	38
2.4 Three Candidate TBDMIs	43
2.5 Residual Concerns and a Fourth TBDMI	46
2.6 Results	49
2.7 Going Forward (Final Caveats)	51
3 Using TBDMIs In Tanker Basing Analysis	57
3.1 Introduction	57
3.2 Location Routing and Scheduling Models	58
3.3 Tanker Basing	60

3.4	Comparing Data Sets	68
3.5	Suggestions for Further Research	72
4	Optimizing Tanker Training Schedules	74
4.1	Introduction	74
4.2	A Scheduling Model	75
4.3	Results	77
4.4	Directions of Future Research	79
	References	80
	Vita	82

List of Figures

1.1	The world and plane reference coordinate systems.	4
1.2	Division of flight path velocity into orthogonal world reference velocities.	5
1.3	Division of Weight into Orthogonal Plane Reference Coordinates	6
1.4	Relevant forces of powered flight.	7
1.5	Definition of α (angle of attack)	11
1.6	Typical Layout of Specific Range Data	17
1.7	Conversion of Specific Range Data into Δt values	18
1.8	Conversion of Δt values into Time Series	18
1.9	Set \mathcal{P} of Mach Altitude Pairs used in model run.	23
1.10	Estimation errors mapped by Mach and altitude.	24
1.11	Estimation errors mapped by Mach and altitude zoomed in on range of cruising altitude and Mach.	25
1.12	An output of the results when the algorithm is modified to find a parameter vector $[\widehat{A}\widehat{B}\widehat{C}\widehat{D}]_{zv}$ for each Mach, altitude pair separately.	26
1.13	Characteristic employment AR mission tanker sortie.	27
2.1	Original Six Region Tanker Basing Demand Mismatch Map	34
2.2	The traditional 6 region map, and a boundary scheme that concentrates demand into two regions	36
2.3	A grid of discrete locations generated over CONUS	38
2.4	Illustrating points of discontinuity generated by a simple indicator function	39
2.5	The percent share of the tanker fleet within M miles of two example locations	40
2.6	Illustration of the round trip distance between a location and an area of AR activity	42
2.7	Actual Supply Score viewed as the Ideal Demand Score	43
2.8	Actual Demand Score viewed as the Ideal Supply Score	44
2.9	A situation where the demand signal will outlast the supply signal	46
2.10	Example of two different supply structures with the same supply scores	47
2.11	Example of tankers located just outside a locations M mile radius	48
2.12	Results of the 6TBDMI	50
2.13	Results of the new TBDMIs for $M = 500$	52
2.14	Results of the new TBDMIs for $M = 750$	53
2.15	Results of the new TBDMIs for $M = 1000$	54
2.16	Results of the new TBDMIs for $M = 1250$	55

3.1	Air fields at which the FY12 tanker basing plan locates tanker aircraft	61
3.2	Basing plans generated by the Location Routing Model	62
3.3	M=500 Demand Score Maps for the three different time periods . . .	63
3.4	M=750 Demand Score Maps for the three different time periods . . .	64
3.5	Results from optimal scheduling model	65
3.6	TBDMI ₁ Maps Generated by the Opt 0708 Basing Strategy	66
3.7	TBDMI ₁ Maps Generated by the FY12 Basing Strategy	67
3.8	Decomposition of demand for AR support by priority level	68
3.9	TBDMI ₁ maps for the fifth basing strategy	70
3.10	TBDMI ₁ maps for the sixth basing strategy	71
4.1	Potential quarterly savings	78
4.2	Potential annual savings	78

Chapter 1

Optimal Control Formulations of Tanker Sortie Planning Problems

1.1 Introduction

When modeling aerial refueling operations it is important to remember that fuel is both a commodity (one of the things being delivered), and a resource (one of the things that makes a delivery possible). Moreover, it can be shown that the rate at which a plane consumes fuel increases quadratically with the amount of fuel loaded onto it. Consequently detailed flight planning is an essential component of any effort to model AR operations. Currently, state of the art mobility simulation and optimization packages, and the best tanker analysts in the Air Force, compute fuel consumption and associated flight planning problems with the Portable Flight Planning System (PFPS) or algorithms that iterate over a specific range table. These are the default tools because they are extremely accurate and very easy to understand. That being said, they have serious limitations. For example, PFPS only generates one flight plan at a time. Consequently, it is not of any practical use to someone who needs to input the costs of 100,000 different flight plans into an optimization or simulation model. Meanwhile, algorithms that iterate over a specific range table consume large amounts of processing time and memory. In addition to this, there is no indication that PFPS or any of the iterative methods make any attempt to construct optimal flight paths. That job rests completely on the judgment, skills, and experience of the end user.

In spite of the importance of realistic fuel flow calculations, none of the recent works completed at Washington University, The Air Force Institute of Technology, or The

University of Texas Austin have adequately touched on the subject ([11], [17], [14], [3], [9], [12]).

The earliest and only documented attempt was made in [14] by Russina and Ruthsatz (see equation (1.1)). They model fuel flow with a quadratic polynomial in altitude (ALT), true airspeed (TAS), and weight (WGT), but fail to provide any justification for choosing this model or details about the data they used to estimate their coefficients. Furthermore, they do not provide any insight into the “goodness” of their model’s fit.

$$\begin{aligned} \dot{W} = & \alpha_2(ALT)^2 + \alpha_1(ALT) + \alpha_0 + \dots \\ & \beta_2(TAS)^2 + \beta_1(TAS) + \beta_0 + \dots \\ & \gamma_2(WGT)^2 + \gamma_1(WGT) + \gamma_0 \end{aligned} \tag{1.1}$$

If, as might be expected, they fit their coefficients with linear regression over specific range, or some other type of first difference data¹ it is doubtful they obtained coefficients that fit the data well. Meanwhile, there is no indication that they solved the differential equation in gross weight, or that they fit their coefficients using estimates of a derivative constructed from time series data generated by iterating over specific range data.

The next best effort was probably put forth in [20] by a MITRE contractor named Kirk Yost. Yost starts with a quadratic polynomial that includes interaction terms but eventually boils it down to a Riccati differential equation in weight. Although Yost solves this equation for a function of weight with respect to time, the motivation of his work seems less focused on estimating parameters than it does on replacing iterative methods with a closed formula. Thus, in spite of the fact that Yost derives a valid function for W with respect to time, it seems as if he continued to use parameters estimated from specific range data for the quadratic fuel flow model. Whatever the case may be, the general lack of enthusiasm for Dr. Yost’s model indicates that his results were not as accurate as it was hoped they would be.

¹Given a Mach, altitude, and current gross weight, specific range data provides the number of nautical miles a plane will fly in the time it takes to burn 1000 lbs of fuel. A much more detailed description of specific range data is given in section 1.5.

The goal of this chapter is to address the current the situation by laying the necessary foundation for future work in this area. Specifically this chapter:

- Constructs a closed formula for the rate of fuel consumption from first principles
- Presents a technique that can be used to estimate parameter values from readily available data
- Develops an optimal control formulation of the tanker sortie fuel planning problem

Finally while studying these systems it will be reasonable to assume that a plane's gross weight only changes with fuel consumption (or fuel offload). Consequently fuel weight and gross weight can be used interchangeably. Thus the naive objective of the first section of this chapter will be to find a function f which generates the instantaneous change in gross weight given the current gross weight, altitude, and airspeed.

$$\dot{W} = f(W, Z, V) \tag{1.2}$$

1.2 The Basic Mechanics of Powered Flight

An essential component of solving flight planning problems with analytic methods is a formula for a plane's instantaneous rate of fuel consumption with respect to its gross weight (W), altitude (Z), and true airspeed (V). Such a formula will define the dynamics of the systems discussed in later sections and provide a means to control those systems.

A theoretical foundation of aircraft fuel consumption can be derived from the mechanics of powered flight using one of two coordinate systems: world reference coordinates and plane reference coordinates. World reference coordinates use the plane's "straight line" ground path as the positive x axis and altitude as the z axis. Meanwhile plane reference coordinates use the ray generated by the velocity vector of a plane's center of gravity as the positive horizontal axis. Ultimately flight planning problems

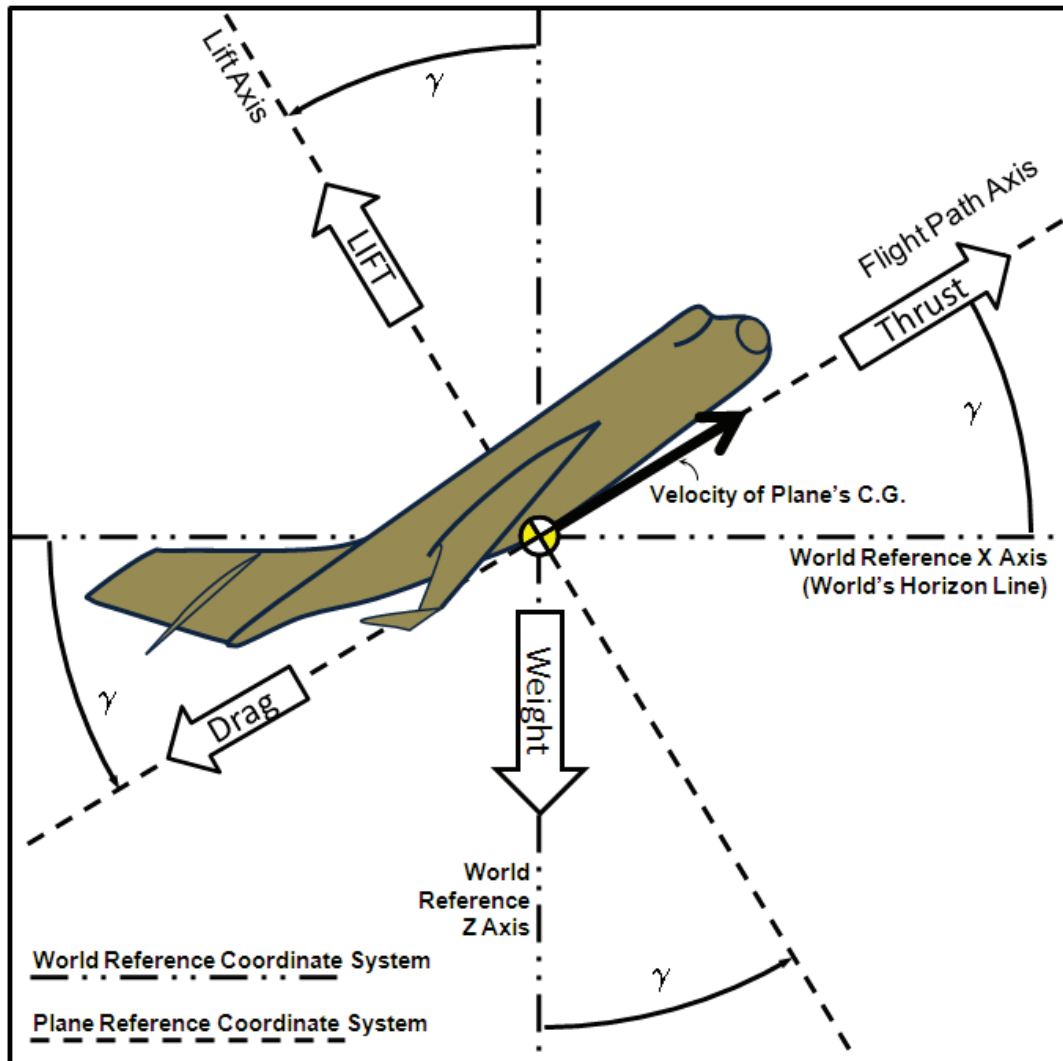


Figure 1.1: The world and plane reference coordinate systems.

will be solved in world reference coordinates, however three of the four forces acting on powered flight (thrust, lift and drag) are either normal to or lie along a plane's flight path². Consequently it will be useful to develop this theory in terms of both coordinate systems.

The relationship between the two systems is given by the projection of a plane's velocity vector onto the x and z axes of the world reference coordinate system. Specifically, define V to be the magnitude of the velocity of a plane along its flight path and let

²According to Lan and Roskam [10] for most planes the force of thrust is very nearly in line with a plane's velocity vector under normal flying conditions.

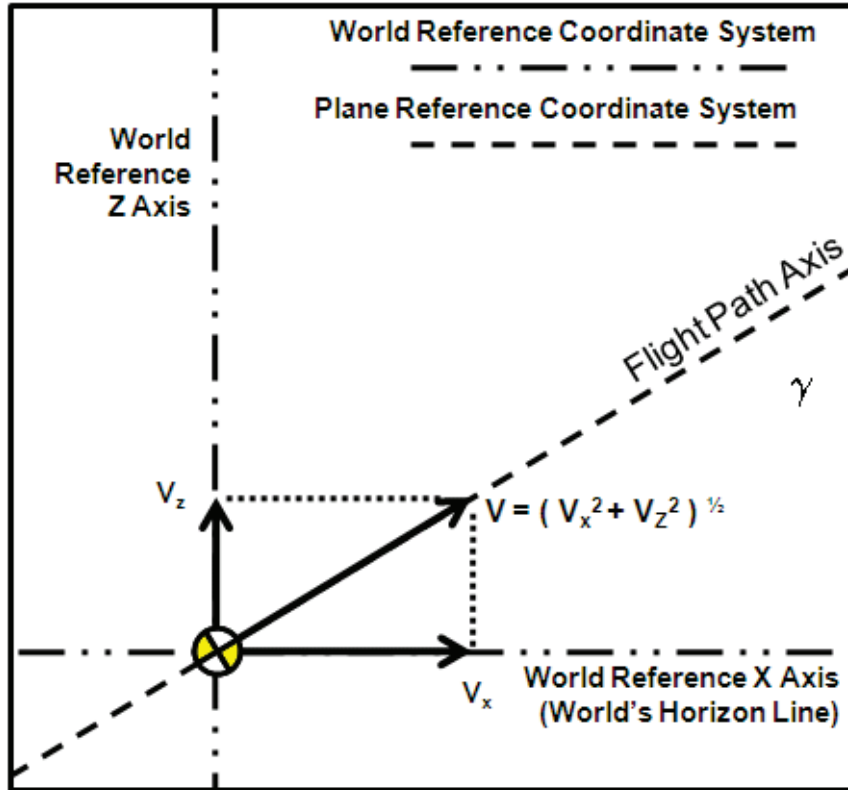


Figure 1.2: Division of flight path velocity into orthogonal world reference velocities.

V_x and V_z be the magnitudes of the orthogonal components of its velocity in world reference coordinates. Then equations (1.3) through (1.6) define identities which can be used to go back and forth between the two systems.

$$V = (V_x^2 + V_z^2)^{\frac{1}{2}} \quad (1.3)$$

$$\cos \gamma = \frac{V_x}{(V_x^2 + V_z^2)^{\frac{1}{2}}} \quad (1.4)$$

$$\sin \gamma = \frac{V_z}{(V_x^2 + V_z^2)^{\frac{1}{2}}} \quad (1.5)$$

$$\tan \gamma = \frac{V_z}{V_x} \quad (1.6)$$

For example, consider the force generated by the weight of the aircraft. This force can be divided into one force which is exerted along a plane's flight path, and another

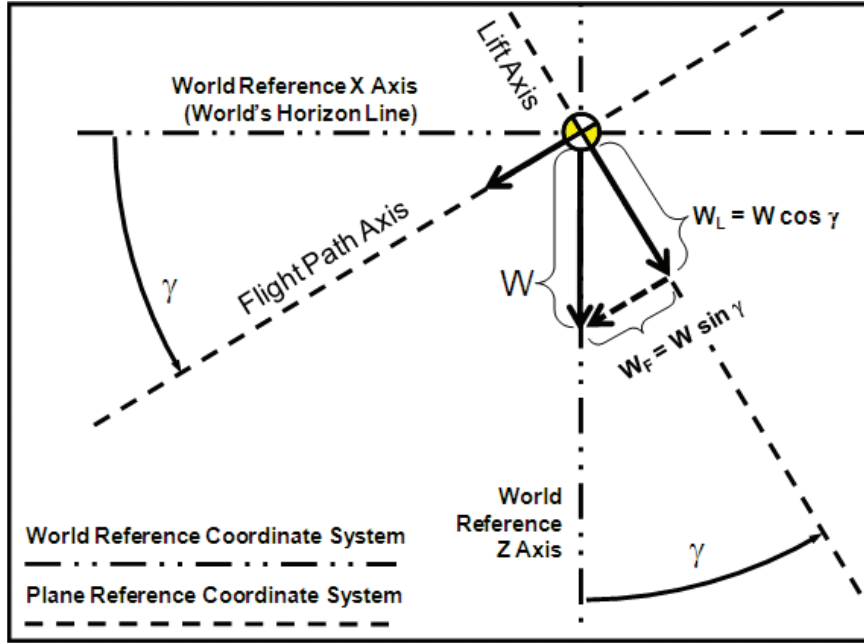


Figure 1.3: Division of Weight into Orthogonal Plane Reference Coordinates

which is exerted in a direction normal to a plane's flight path. Specifically let W be the magnitude of the force generated by the weight of an aircraft along the z -axis, let W_F be the magnitude of the component force exerted along a plane's flight path, and let W_L be the magnitude of the component force exerted normal to a plane's flight path. Then $W_F = W \sin \gamma$ and $W_L = W \cos \gamma$. From this and the above identities, it is possible to generate the identities given by equations (1.7) and (1.8).

$$W_F = \frac{WV_z}{(V_x^2 + V_z^2)^{\frac{1}{2}}} \quad (1.7)$$

$$W_L = \frac{WV_x}{(V_x^2 + V_z^2)^{\frac{1}{2}}} \quad (1.8)$$

It is now possible to write out the equations of flight in terms of forces which are either exerted along a plane's flight path or in a direction normal to a plane's flight path.

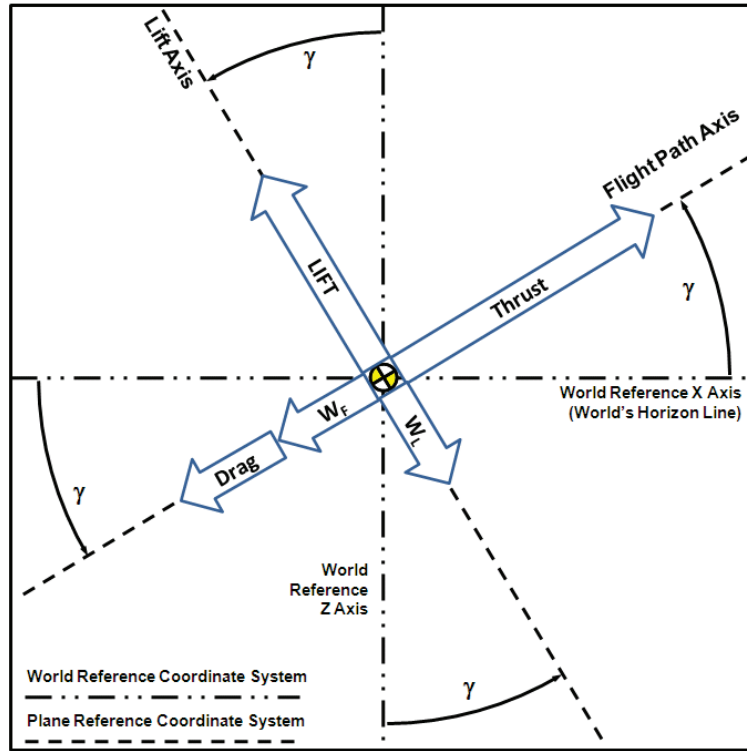


Figure 1.4: Relevant forces of powered flight.

Let T , D , and L be the magnitudes of the forces of thrust, drag and lift (respectively). Then the equations of zero acceleration flight are given by equations (1.9) and (1.10).

$$T = D + W_F \quad (1.9)$$

$$L = W_L \quad (1.10)$$

When the forces in these equations are not balanced a plane in flight will experience some form of acceleration. Let g be the magnitude of the force due to gravity, let Y_1 be the magnitude of a plane's acceleration along its flight path, and let Y_2 be the magnitude of a plane's acceleration along its lift axes. Then the identities in equations (1.11) and (1.12) can be derived from Newton's laws of motion.

$$\frac{W}{g}Y_1 = T - D - W_F \quad (1.11)$$

$$\frac{W}{g}Y_2 = L - W_L \quad (1.12)$$

A similar set of identities can be constructed when the relevant forces are projected into world reference coordinates. These are given in equations (1.13) and (1.14).

$$\frac{W}{g}\dot{V}_x = (T - D - W_F) \cos \gamma + (W_L - L) \sin \gamma \quad (1.13)$$

$$\frac{W}{g}\dot{V}_z = (T - D - W_F) \sin \gamma + (L - W_L) \cos \gamma \quad (1.14)$$

These last four equations can be combined and factored to yield a very useful system of two equations in two unknowns.

$$\begin{bmatrix} \dot{V}_x \\ \dot{V}_z \end{bmatrix} = \begin{bmatrix} \cos \gamma & -\sin \gamma \\ \sin \gamma & \cos \gamma \end{bmatrix} \begin{bmatrix} Y_1 \\ Y_2 \end{bmatrix} \quad (1.15)$$

Since the matrix in this system is non-singular for every angle γ it is possible to express Y_1 and Y_2 and by extension equations (1.11) and (1.12) in terms of previously defined physical quantities.

$$\begin{bmatrix} Y_1 \\ Y_2 \end{bmatrix} = \begin{bmatrix} \cos \gamma & \sin \gamma \\ -\sin \gamma & \cos \gamma \end{bmatrix} \begin{bmatrix} \dot{V}_x \\ \dot{V}_z \end{bmatrix} \quad (1.16)$$

To get Y_1 , consider the top row of equation (1.16) along with equations (1.4) and (1.5):

$$Y_1 = (\dot{V}_x \cos \gamma + \dot{V}_z \sin \gamma) = \frac{\dot{V}_x V_x + \dot{V}_z V_z}{(V_x^2 + V_z^2)^{\frac{1}{2}}} \quad (1.17)$$

Also, recall from equation (1.3) that $V = (V_x^2 + V_z^2)^{\frac{1}{2}}$ and note that differentiating both sides of this equation with respect to t yields the identity in equation (1.18).

$$\dot{V} = \frac{V_x \dot{V}_x + V_z \dot{V}_z}{(V_x^2 + V_z^2)^{\frac{1}{2}}} \quad (1.18)$$

Thus equations (1.17) and (1.18) imply that $Y_1 = \dot{V}$.

$$Y_1 = \dot{V} \quad (1.19)$$

To get Y_2 consider the bottom row of equation (1.16) along with equations (1.4) and (1.5):

$$\begin{aligned} Y_2 &= -\dot{V}_x \sin \gamma + \dot{V}_z \cos \gamma \\ &= \frac{-\dot{V}_x V_z + \dot{V}_z V_x}{(V_x^2 + V_z^2)^{\frac{1}{2}}} \\ &= (V_x^2 + V_z^2)^{\frac{1}{2}} \frac{\dot{V}_z V_x - V_z \dot{V}_x}{(V_x^2 + V_z^2)} \end{aligned} \quad (1.20)$$

Also, recall from equation (1.6) that $\tan \gamma = \frac{V_z}{V_x}$. This implies that $\gamma = \tan^{-1} \left(\frac{V_z}{V_x} \right)$. Finally, note that differentiating both sides of this expression for γ with respect to t yields the identity in equation (1.21).

$$\dot{\gamma} = \frac{\frac{d}{dt} \left[\frac{V_z}{V_x} \right]}{1 + \left(\frac{V_z}{V_x} \right)^2} = \frac{(\dot{V}_z V_x - V_z \dot{V}_x) / V_x^2}{1 + \left(\frac{V_z}{V_x} \right)^2} = \frac{\dot{V}_z V_x - V_z \dot{V}_x}{V_x^2 + V_z^2} \quad (1.21)$$

Thus equations (1.20) and (1.21) imply that $Y_2 = V \dot{\gamma}$.

$$Y_2 = V \dot{\gamma} \quad (1.22)$$

Consequently equations (1.11) and (1.12) can be written completely in terms of previously defined physical quantities

$$\dot{V} \left(\frac{W}{g} \right) = T - D - W_F \quad (1.23)$$

$$V \dot{\gamma} \left(\frac{W}{g} \right) = L - W_L \quad (1.24)$$

These last two equations provide half of the fuel flow model's theoretical foundations. The next quarter of the model is provided by the ratio between pounds of fuel burned per hour and the maximum pounds of thrust produced by burning fuel at that rate.

$$T_{SFC} = \frac{\dot{W}}{T} \quad (1.25)$$

This ratio is known as *Thrust Specific Fuel Consumption* (T_{SFC}) and is believed to be a function of altitude and airspeed. It will be more useful in the current exercise when expressed as in equation (1.26).

$$\dot{W} = T_{SFC}(Z, V) T \quad (1.26)$$

Finally, it will be difficult to derive a fuel flow formula without approximating a relationship between lift and drag. Let L and D be the magnitudes of the forces of lift and drag. These magnitudes are given by equations (1.27) and (1.28).

$$L = (\rho(Z) V^2 S) C_L \quad (1.27)$$

$$D = (\rho(Z) V^2 S) C_D \quad (1.28)$$

where $\rho(Z)$ is the density of the atmosphere at altitude Z , V is the airplane's true airspeed, S is the surface area of the plane's lifting surfaces, C_L is the coefficient of

lift, and C_D is the coefficient of drag. In [6] Hale writes that the coefficients of lift and drag change continuously with the Mach number, the Reynolds number, and the angle α between a plane's wing chord and its velocity vector.

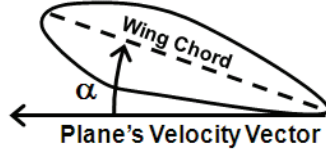


Figure 1.5: Definition of α (angle of attack)

$$C_L = C_L(\alpha, M, Re)$$

$$C_D = C_D(\alpha, M, Re)$$

Hale also states that C_L is a monotonically increasing function of α up to the stall point $C_{L_{max}}$. Thus, if it is assumed that a plane will not fly beyond this point, it is possible to write α as a function of C_L . Consequently it is possible to write C_D as a function of C_L , the Mach number, and the Reynolds number.

$$C_D = C_D(C_L, M, Re) \tag{1.29}$$

Approximating this function with a second order Taylor expansion around the point (C_{L_0}, C_{D_0}) where $C_{D_0} = C_{D_{min}}$ yields the following expression

$$\begin{aligned} C_D(C_L; M, Re) &\dots \\ &\dots \approx C_D(C_{L_0}; M, Re) + C'_D(C_{L_0}; M, Re)(C_L - C_{L_0}) + \frac{1}{2}C''_D(C_{L_0}; M, Re)(C_L - C_{L_0})^2 \\ &\dots = C_D(C_{L_0}; M, Re) + \frac{1}{2}C''_D(C_{L_0}; M, Re)(C_L - C_{L_0})^2 \\ &\dots = C_{D_0}(M, Re) + K(M, Re)(C_L - C_{L_0})^2 \end{aligned} \tag{1.30}$$

It is assumed that $C'_D(C_{L_0}; M, Re) = 0$ for all values of M and Re because this is a first order necessary condition of a minimum. Hale writes that the coefficients

$C_{D_0}(M, Re)$ and $K(M, Re)$ can in practice be regarded as constants. Finally, although no author explicitly states that C_{L_0} can be regarded as a constant, it has not been treated otherwise in any of the aircraft performance text books which have thus far been reviewed. Thus it is assumed that the following is a reasonable, if not a good approximation of the functional relationship between C_D and C_L for values of C_L up to $C_{L_{\max}}$.

$$C_D \approx C_{D_0} + K (C_L - C_{L_0})^2 \quad (1.31)$$

This equation is known as the *parabolic drag polar equation* and will be used in an expanded form

$$C_D \approx (K) C_L^2 - (2KC_{L_0}) C_L + (C_{D_0} + KC_{L_0}^2) \quad (1.32)$$

Finally combining equations (1.27), (1.28), and (1.32) it follows that

$$\begin{aligned} D &= (\rho(Z)V^2S) \left[K \left(\frac{L}{\rho(Z)V^2S} \right)^2 - (2KC_{L_0}) \left(\frac{L}{\rho(Z)V^2S} \right) + (C_{D_0} + KC_{L_0}^2) \right] \\ &= \left(\frac{K}{\rho(Z)V^2S} \right) L^2 - (2KC_{L_0}) L + (\rho(Z)V^2S) (C_{D_0} + KC_{L_0}^2) \end{aligned} \quad (1.33)$$

1.3 The Rate of Fuel Consumption

It is now possible to derive a general model for the rate at which a plane consumes fuel while in flight. This model is based on the balance of forces identities culminating in equations (1.23) and (1.24), the relationship between thrust and fuel flow given in equation (1.26), and the relationship between lift and drag given in equation (1.33).

First note that equation (1.23) can be re-written so that thrust is expressed as a function of drag, gross weight, acceleration along the flight path, and the angle of the flight path with respect to the world's horizon. Doing so generates equation (1.34).

$$T = D + W \left(\frac{\dot{V}}{g} + \sin \gamma \right) \quad (1.34)$$

Subbing this into equation (1.26) yields equation (1.35).

$$\dot{W} = T_{SFC}(Z, V) \left[D + W \left(\frac{\dot{V}}{g} + \sin \gamma \right) \right] \quad (1.35)$$

Next note that equation (1.24) can be re-written so that lift is expressed as a function of weight, acceleration along the flight path, the rate of change in the angle of the flight path with respect to time, and the angle of the flight path with respect to the world's horizon. Doing so generates equation (1.36).

$$L = W \left(\frac{V\dot{\gamma}}{g} + \cos \gamma \right) \quad (1.36)$$

Subbing this into equation (1.33) yields equation (1.37).

$$D = \dots$$

$$\left[\frac{K \left(\frac{V\dot{\gamma}}{g} + \cos \gamma \right)^2}{\rho(Z) V^2 S} \right] W^2 - (2KC_{L_0}) \left(\frac{V\dot{\gamma}}{g} + \cos \gamma \right) W + (\rho(Z) V^2 S) (C_{D_0} + KC_{L_0}^2) \quad (1.37)$$

Finally, subbing equation (1.37) into equation (1.35) yields equation (1.38).

$$\dot{W} = T_{SFC}(Z, V) \left[\alpha_1 W^2 + \alpha_2 W + \alpha_3 \right] \quad (1.38)$$

where:

$$\alpha_1 = \frac{K \left(\frac{V\dot{\gamma}}{g} + \cos \gamma \right)^2}{\rho(Z) V^2 S} \quad (1.39)$$

$$\alpha_2 = \left(\frac{\dot{V}}{g} + \sin \gamma \right) - (2KC_{L_0}) \left(\frac{V\dot{\gamma}}{g} + \cos \gamma \right) \quad (1.40)$$

$$\alpha_3 = \left(\rho(Z) V^2 S \right) \left(C_{D_0} + KC_{L_0}^2 \right) \quad (1.41)$$

Next note that each of these coefficients can be expressed as functions of Z , V_x , \dot{V}_x , V_z , and \dot{V}_z . First consider the following

$$\begin{aligned} \frac{V\dot{\gamma}}{g} + \cos \gamma &= \left(\frac{(V_x^2 + V_z^2)^{\frac{1}{2}}}{g} \right) \left(\frac{\dot{V}_z V_x - V_z \dot{V}_x}{V_x^2 + V_z^2} \right) + \left(\frac{V_x}{(V_x^2 + V_z^2)^{\frac{1}{2}}} \right) \\ &= \left(\frac{\dot{V}_z V_x - V_z \dot{V}_x}{g (V_x^2 + V_z^2)^{\frac{1}{2}}} \right) + \left(\frac{g V_x}{g (V_x^2 + V_z^2)^{\frac{1}{2}}} \right) \\ &= \frac{\dot{V}_z V_x - V_z \dot{V}_x + g V_x}{g (V_x^2 + V_z^2)^{\frac{1}{2}}} \end{aligned}$$

Thus α_1 can be written as

$$\begin{aligned} \alpha_1 &= \frac{K \left(\frac{V\dot{\gamma}}{g} + \cos \gamma \right)^2}{\rho(Z) V^2 S} \\ &= \frac{K \left(\frac{\dot{V}_z V_x - V_z \dot{V}_x + g V_x}{g (V_x^2 + V_z^2)^{\frac{1}{2}}} \right)^2}{\rho(Z) (V_x^2 + V_z^2) S} \\ &= \frac{K \left(\dot{V}_z V_x - V_z \dot{V}_x + g V_x \right)^2}{\rho(Z) g^2 (V_x^2 + V_z^2)^2 S} \end{aligned} \quad (1.42)$$

Additionally α_2 can be written as

$$\begin{aligned}\alpha_2 &= \left(\frac{\dot{V}}{g} + \sin \gamma \right) - (2KC_{L_0}) \left(\frac{V\dot{\gamma}}{g} + \cos \gamma \right) \\ &= \frac{(\dot{V}_x V_x + \dot{V}_z V_z + gV_z) - (2KC_{L_0}) (\dot{V}_z V_x - V_z \dot{V}_x + gV_x)}{g(V_x^2 + V_z^2)^{\frac{1}{2}}}\end{aligned}\quad (1.43)$$

And finally α_3 can be written as

$$\alpha_3 = [\rho(Z) (V_x^2 + V_z^2) S] [C_{D_0} + KC_{L_0}^2] \quad (1.44)$$

Thus a model for the plane's fuel flow, with respect to its current state is given by

$$\frac{d}{dt} \begin{bmatrix} W \\ X \\ Z \\ V_x \\ V_z \end{bmatrix} = \begin{bmatrix} f(W, Z, V_x, V_z, \dot{V}_x, \dot{V}_z) \\ V_x \\ V_z \\ \dot{V}_x \\ \dot{V}_z \end{bmatrix} \quad (1.45)$$

where

$$f(W, Z, V_x, V_z, \dot{V}_x, \dot{V}_z) = T_{SFC}(Z, V_x, V_z) [\alpha_1 W^2 + \alpha_2 W + \alpha_3] \quad (1.46)$$

and

$$\alpha_1 = \frac{K (\dot{V}_z V_x - V_z \dot{V}_x + gV_x)^2}{\rho(Z) g^2 (V_x^2 + V_z^2)^2 S} \quad (1.47)$$

$$\alpha_2 = \frac{(\dot{V}_x V_x + \dot{V}_z V_z + gV_z) - (2KC_{L_0}) (\dot{V}_z V_x - V_z \dot{V}_x + gV_x)}{g(V_x^2 + V_z^2)^{\frac{1}{2}}} \quad (1.48)$$

$$\alpha_3 = [\rho(Z) (V_x^2 + V_z^2) S] [C_{D_0} + KC_{L_0}^2] \quad (1.49)$$

1.4 Further Notation

In later sections it will be convenient to identify the fuel flow model as it runs backwards in time with its own special notation. Let $\xi(t)$ be the state vector of this model. Then

$$\xi(t) \equiv [W(-t), X(-t), Z(-t), V_x(-t), V_z(-t)]^T \quad (1.50)$$

and

$$\frac{d}{dt}\xi(t) = \begin{bmatrix} -f(W(-t), Z(-t), V_x(-t), V_z(-t), \dot{V}_x(-t), \dot{V}_z(-t)) \\ -V_x(-t) \\ -V_z(-t) \\ -\dot{V}_x(-t) \\ -\dot{V}_z(-t) \end{bmatrix} \quad (1.51)$$

Let $u_1(t) = -\dot{V}_x(-t)$ and $u_2(t) = -\dot{V}_z(-t)$. Then, with some relabeling, the fuel flow model can be re-written in terms of the components of a state vector ξ and a control vector $u = [u_1, u_2]^T$.

$$\frac{d}{dt}\xi(t) = \begin{bmatrix} -f(\xi_1(t), \xi_3(t), \xi_4(t), \xi_5(t), u_1(t), u_2(t)) \\ -\xi_4(t) \\ -\xi_5(t) \\ u_1(t) \\ u_2(t) \end{bmatrix} \quad (1.52)$$

For convenience, let

$$F(\xi, u) = \begin{bmatrix} -f(\xi_1, \xi_3, \xi_4, \xi_5, u_1, u_2) \\ -\xi_4 \\ -\xi_5 \\ u_1 \\ u_2 \end{bmatrix} \quad (1.53)$$

Then we can simply write $\dot{\xi} = F(\xi, u)$.

1.5 Estimators For Unknown Coefficients

The model derived in the previous sections is of little practical use without reasonable estimates of the area of the lifting surfaces S , the minimum drag coefficient C_{D_0} , the lift coefficient corresponding to the minimum drag coefficient C_{L_0} , the second order Taylor coefficient of the drag polar K , or a function for thrust specific fuel consumption $T_{SFC}(Z, V)$. The only data readily available to derive these estimates is called *Specific Range Data*.

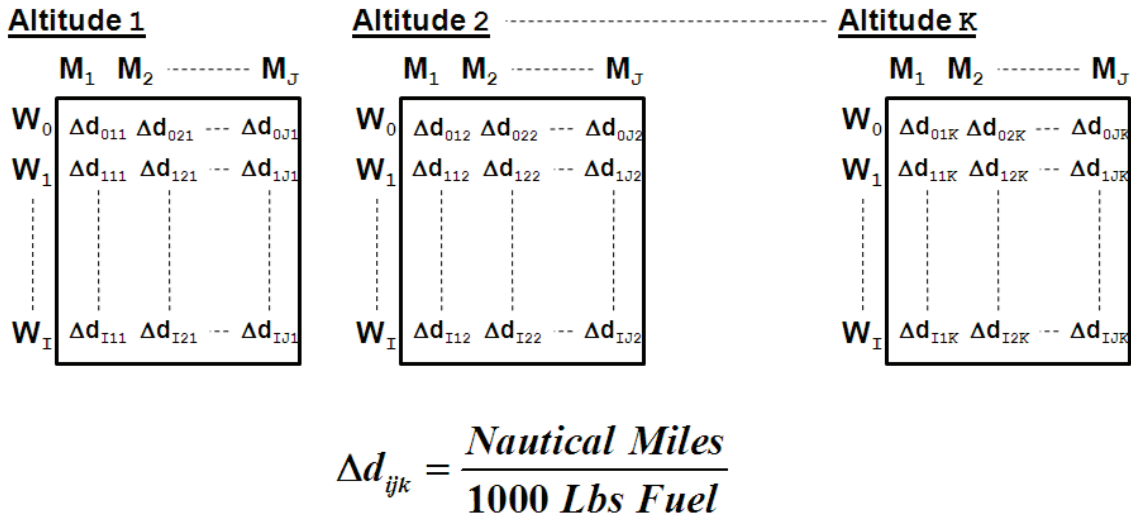
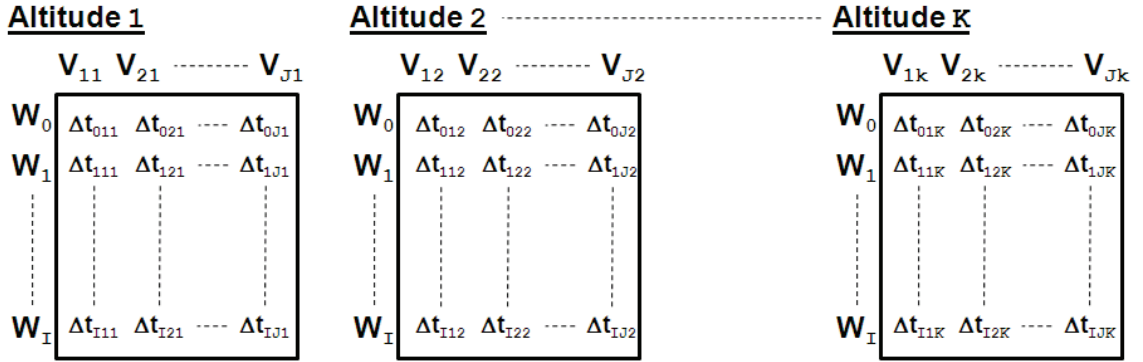


Figure 1.6: Typical Layout of Specific Range Data

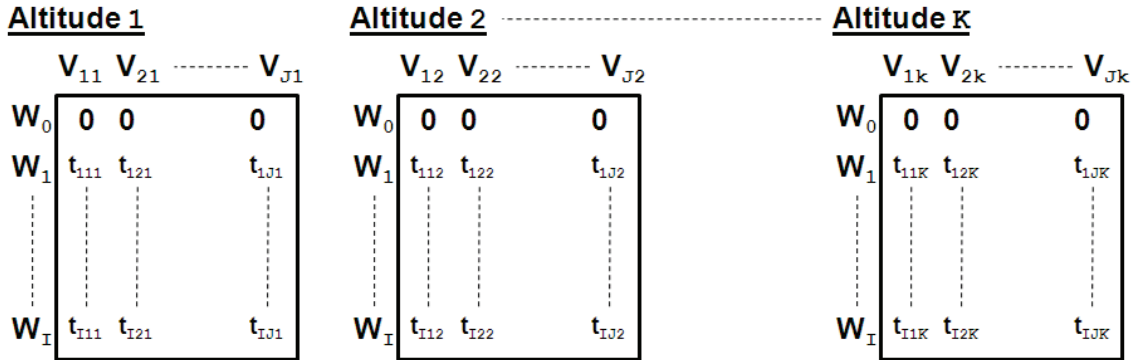
Specific range data is typically organized in large lookup tables which, for a given altitude, Mach number, and gross weight, provide the number of nautical miles a plane can travel per 1000 lbs of fuel. Note that altitude and Mach are held constant over each column of data. Therefore each column of data is associated with a constant true airspeed. Consequently, it is possible to convert each specific range data point into the amount of time it takes to burn 1000 lbs of fuel given a constant altitude, airspeed, and a starting weight. The converted data can then be used to generate time series which approximate the amount of time that would pass for a given change in a plane's gross weight if it flew at a constant altitude and airspeed, and had a starting weight W_0 . Finally these time series can be used to estimate the values of the unknown parameters. That is, of course, if it is possible to solve the differential equation defined by equations (1.38) through (1.41).



$$V_{jk} = M_j * (\text{Speed of Sound @ Altitude } Z_k)$$

$$\Delta t_{ijk} = \frac{\text{Minutes}}{1000 \text{ Lbs Fuel}}$$

Figure 1.7: Conversion of Specific Range Data into Δt values



$$t_{ijk} = \begin{cases} 0 & i = 0 \\ t_{(i-1)jk} + \Delta t_{(i-1)jk} & i > 0 \end{cases}$$

(Assumes $W_i - W_{(i+1)} = 1000 \text{ lbs}$, $i = 0, 1, \dots, I$)

Figure 1.8: Conversion of Δt values into Time Series

It turns out that this is not a difficult thing to do. Recall that the time series generated from the spec range data assume a constant altitude and a constant positive airspeed. Thus along any given column of data, $V_x > 0$ and $V_z = \dot{V}_x = \dot{V}_z = 0$. This implies that $\gamma = \dot{\gamma} = 0$. Thus the differential equation associated with a particular column of data (identified by a choice of altitude z and airspeed v) can be simplified into equation (1.54).

$$\dot{W} = aW^2 - bW + c \quad (1.54)$$

with constant coefficients:

$$a = \frac{T_{SFC}^{zv} K}{\rho(Z) V^2 S} \quad (1.55)$$

$$b = 2T_{SFC}^{zv} K C_{L_0} \quad (1.56)$$

$$c = T_{SFC}^{zv} (\rho(Z) V^2 S) (C_{D_0} + K C_{L_0}^2) \quad (1.57)$$

This is a Riccati equation in W and is easily solved using standard techniques. In particular, the solution to the initial value problem associated with a choice of altitude (Z), airspeed (V), and initial gross weight (W_0) is given by equation (1.58).

$$W(t) = W_0 \left[\frac{\cos(\frac{1}{2}dt) + \left(\frac{W_0 b - 2c}{d W_0}\right) \sin(\frac{1}{2}dt)}{\cos(\frac{1}{2}dt) + \left(\frac{2a W_0 - b}{d}\right) \sin(\frac{1}{2}dt)} \right] \quad (1.58)$$

where

$$d = \sqrt{4ac - b^2} = 2T_{SFC}^{zv} K^{\frac{1}{2}} C_{D_0}^{\frac{1}{2}} \quad (1.59)$$

Careful organization of the terms in the coefficients of the sin functions provide a formula for $W(t)$ parameterized by: W_0 ; Z ; V ; three parameters A , B , and C ; and a value D_{zv} which depends on Z and V . First note that the coefficient of the sin term in the numerator of equation (1.58) can be written as as in equation (1.60).

$$\begin{aligned}
\frac{W_0 b - 2c}{dW_0} &= \frac{W_0 (2T_{SFC}^{zv} K C_{L_0}) - 2 (T_{SFC}^{zv} \rho(Z) V^2 S) (C_{D_0} + K C_{L_0}^2)}{W_0 \left(2T_{SFC}^{zv} K^{\frac{1}{2}} C_{L_0}^{\frac{1}{2}} \right)} \\
&= \frac{W_0 (K C_{L_0}) - (\rho(Z) V^2 S) (C_{D_0} + K C_{L_0}^2)}{W_0 \left(K^{\frac{1}{2}} C_{L_0}^{\frac{1}{2}} \right)} \\
&= \left(\frac{K}{C_{D_0}} \right)^{\frac{1}{2}} - \left(\frac{S (C_{D_0} + K C_{L_0}^2)}{K^{\frac{1}{2}} C_{D_0}^{\frac{1}{2}}} \right) \left(\frac{\rho(Z) V^2}{W_0} \right) \tag{1.60}
\end{aligned}$$

and that the coefficient of the sin term in the denominator of equation (1.58) can be written as in equation (1.61).

$$\begin{aligned}
\frac{2aW_0 - b}{d} &= \frac{2 \left(\frac{T_{SFC}^{zv} K}{\rho(Z) V^2 S} \right) W_0 - 2T_{SFC}^{zv} K C_{L_0}}{2T_{SFC}^{zv} K^{\frac{1}{2}} C_{D_0}^{\frac{1}{2}}} \\
&= \frac{\left(\frac{K}{S} \right) \left(\frac{W_0}{\rho(Z) V^2} \right) - K C_{L_0}}{K^{\frac{1}{2}} C_{D_0}^{\frac{1}{2}}} \\
&= \left(\frac{K}{S^2 C_{D_0}} \right)^{\frac{1}{2}} \left(\frac{W_0}{\rho(Z) V^2} \right) - \left(\frac{K}{C_{D_0}} \right)^{\frac{1}{2}} C_{L_0} \tag{1.61}
\end{aligned}$$

Thus it is possible to re-write equation (1.58) in the following way:

$$W(t) = W_0 \left[\frac{\cos(D_{zv} t) + \left(A - B \frac{\rho(Z) V^2}{W_0} \right) \sin(D_{zv} t)}{\cos(D_{zv} t) + \left(C \frac{W_0}{\rho(Z) V^2} - A \right) \sin(D_{zv} t)} \right] \tag{1.62}$$

where

$$A = \left(\frac{K}{C_{D_0}} \right)^{\frac{1}{2}} C_{L_0} \tag{1.63}$$

$$B = \frac{S(C_{D_0} + KC_{L_0}^2)}{K^{\frac{1}{2}}C_{D_0}^{\frac{1}{2}}} \quad (1.64)$$

$$C = \left(\frac{K}{S^2C_{D_0}}\right)^{\frac{1}{2}} \quad (1.65)$$

$$D_{zv} = \frac{d}{2} = T_{SFC}^{zv}K^{\frac{1}{2}}C_{D_0}^{\frac{1}{2}} \quad (1.66)$$

The advantage of this parameterization is that *the coefficients A , B , C , and a coefficient matrix D_{zv} can be estimated from the time series data* by minimizing the sum of the squared errors,

$$\arg \min_{ABCD_{zv}} \sum_{j=1}^J \sum_{k=1}^K \sum_{i=1}^{I_{jk}} \sum_{h=1}^{H_{ijk}} [W_{hijk} - \widehat{W}_{hijk}(A, B, C, D_{jk})]^2 \quad (1.67)$$

The indices (i, j, k) identify the data series to which a particular data point belongs. Specifically, for a given data series, j is the index of its Mach, k is the index of its altitude, and i is the index of its initial weight. Meanwhile, h identifies the position of a data point within a particular series. Note that the maximum number of initial weights depends on the Mach, altitude pair. This is because some Mach altitude pairs do not support the full range of initial weights.

1.6 Estimation Results

This model was implemented in MATLAB version 7.9.0 using the MATLAB function *nlinfit* along with the following algorithm.

1. Choose a subset \mathcal{P} of supported Mach altitude pairs

2. Choose a subset \mathcal{W} of initial weights to be used with each Mach altitude pair.

3. For each Mach altitude pair in \mathcal{P} and each initial weight in \mathcal{W}
 - 3.1. Check if Mach altitude pair supports initial weight. Move on to next initial weight if current weight is not supported.

 - 3.2. Use current Mach, altitude, and initial weight along with specific range data to construct a time series W_{hijk} .

 - 3.3. Use the Mach, Altitude, and initial weight to build inputs for \widehat{W}_{ijkh} which correspond to the time series.

 - 3.4. Store time series and corresponding inputs in memory.

4. Use the MATLAB function *nlinfit* along with data generated in step 3 to estimate A , B , C , and D_{zv} .

5. For each Mach altitude pair supported by the specific range data set
 - 5.1. For each initial weight that is supported by the Mach, altitude pair construct a time series W_{hijk} and inputs for \widehat{W}_{ijkh} using the estimates for A , B , and C generated in step 4.

 - 5.2 Use the MATLAB function *nlinfit* along with the data generated in the previous steps to estimate D_{zv} for the current Mach altitude pair.

This algorithm was implemented over the spec range data of a narrow body transport jet with the set \mathcal{P} defined in table 1.9. The maximum absolute errors produced over any of the time series associated with a particular Mach altitude pair are mapped in figure 1.10. Figure 1.11 zooms in on the top left corner of figure 1.10 and highlights some absolute errors observed in the neighborhood of typical cruising Machs and

	Flight Level (1000ft)					
Mach	10	15	20	25	30	35
0.40	X	X				
0.42	X	X				
0.44	X	X				
0.46	X	X	X			
0.48	X	X	X			
0.50	X	X	X	X		
0.52	X	X	X	X		
0.54	X	X	X	X		
0.56	X	X	X	X		
0.58	X	X	X	X		
0.60	X	X	X	X	X	
0.62	X	X	X	X	X	
0.64		X	X	X	X	
0.66		X	X	X	X	
0.68		X	X	X	X	
0.70		X	X	X	X	X
0.72			X	X	X	X
0.74			X	X	X	X
0.76			X	X	X	X

Figure 1.9: Set \mathcal{P} of Mach Altitude Pairs used in model run.

altitudes. From these figures two things are clear. First, the maximum absolute error between a value $W(t; A, M, W_0)$ derived from iterating over the associated specific range table and an estimated value $\widehat{W}(t; A, M, W_0)$ is less than 5,000 lbs or less than 2% of the aircraft's maximum ramp weight. Second, the concentration of large errors at the extremes indicates that there might be something wrong with the assumption that C_{D_0} , K , and C_{L_0} are constants.

To check the constant coefficients assumption the algorithm was modified to find a parameter vector $[\widehat{A}\widehat{B}\widehat{C}\widehat{D}]_{zv}$ for each Mach altitude pair. The output of this algorithm is presented in figure 1.12. From this picture it should be clear that *both \widehat{B} and \widehat{C} are strongly affected by Mach, but probably not affected by altitude.* Meanwhile, *\widehat{A} seems to be affected by both Mach and altitude.* Finally note that the maximum absolute errors are now extremely small.

Although the extremely small errors in the second model are highly desirable, allowing all four parameters to vary with Mach and altitude increases the complexity of the

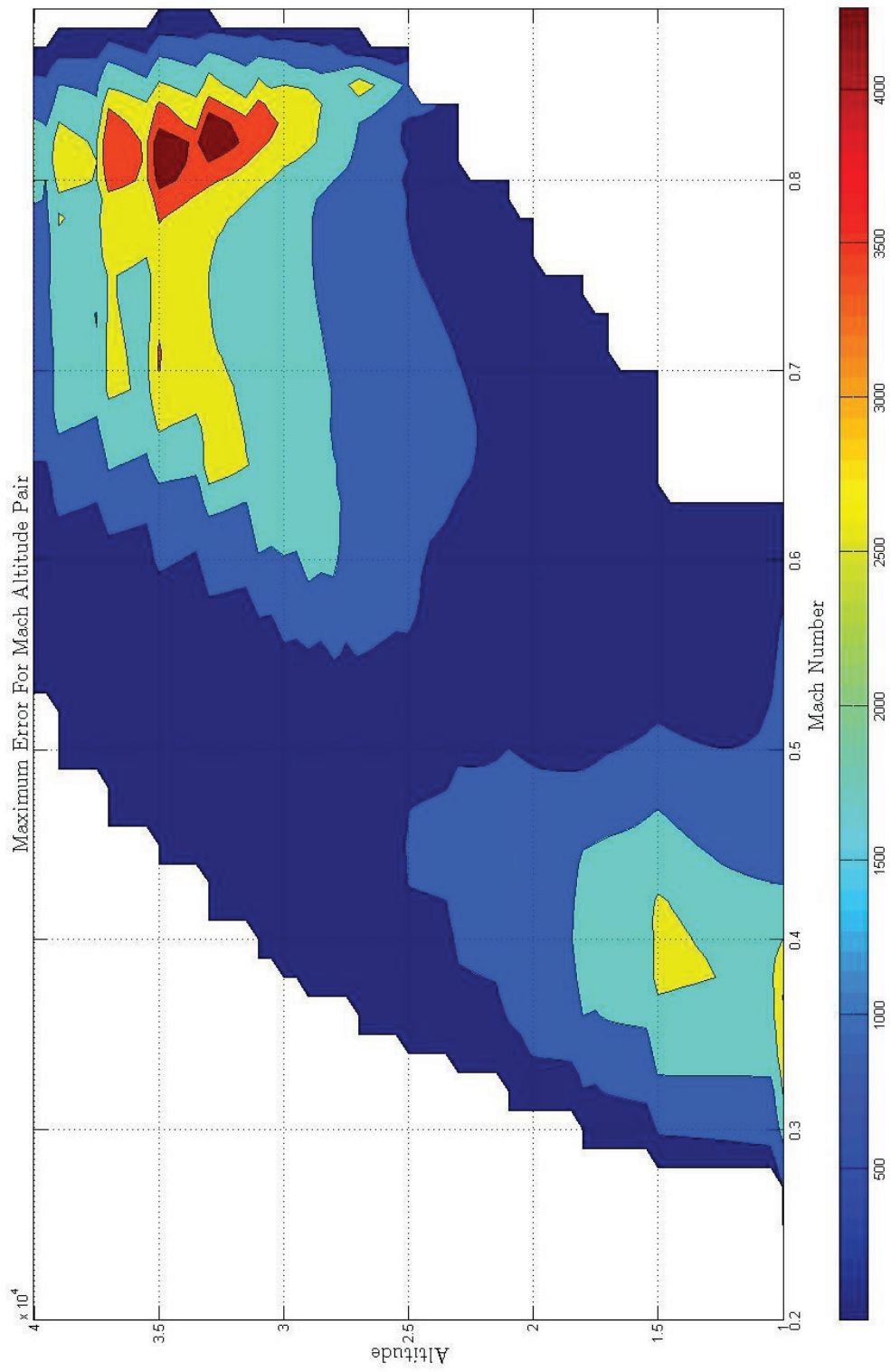


Figure 1.10: Estimation errors mapped by Mach and altitude.

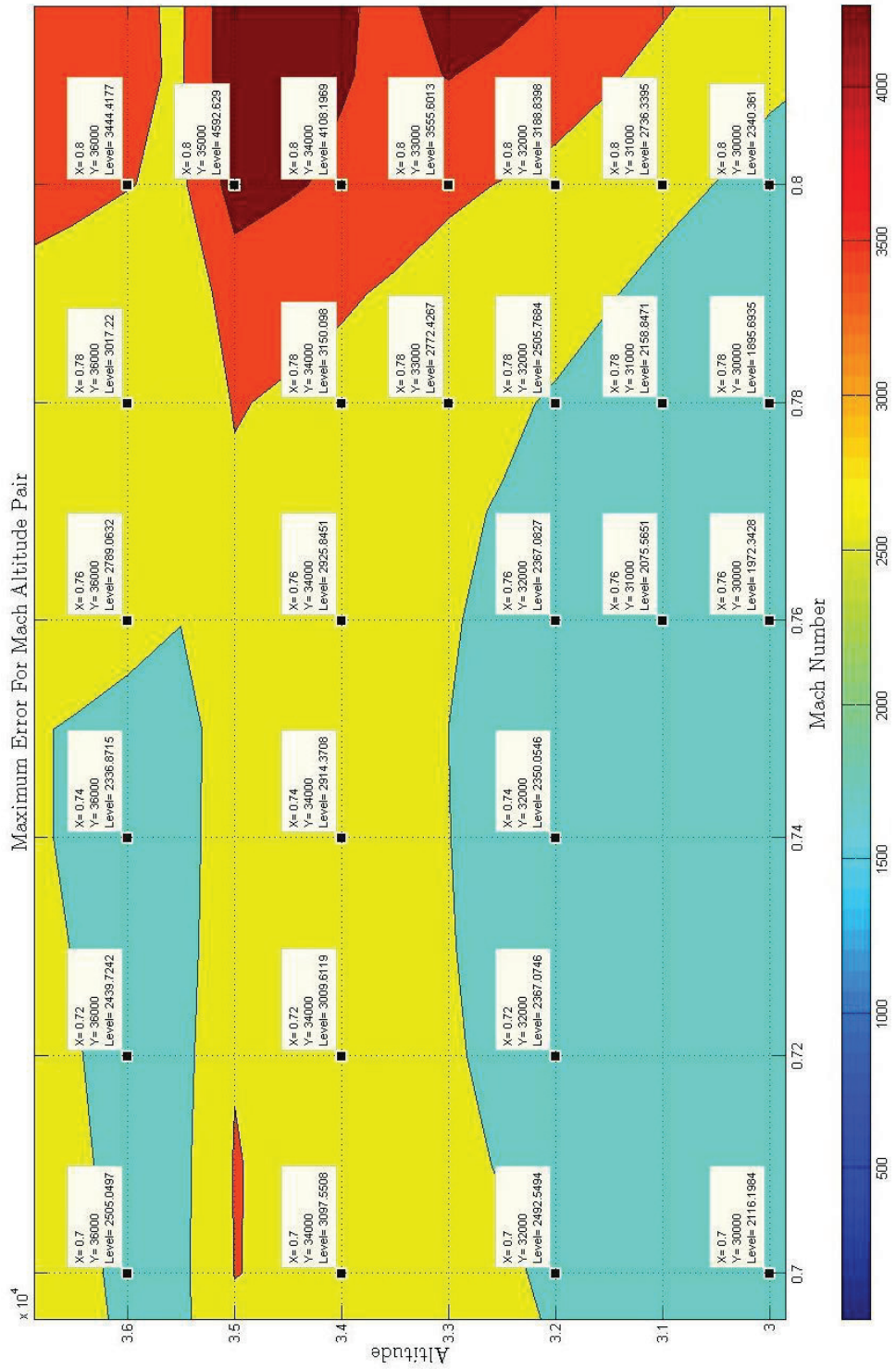


Figure 1.11: Estimation errors mapped by Mach and altitude zoomed in on range of cruising altitude and Mach.

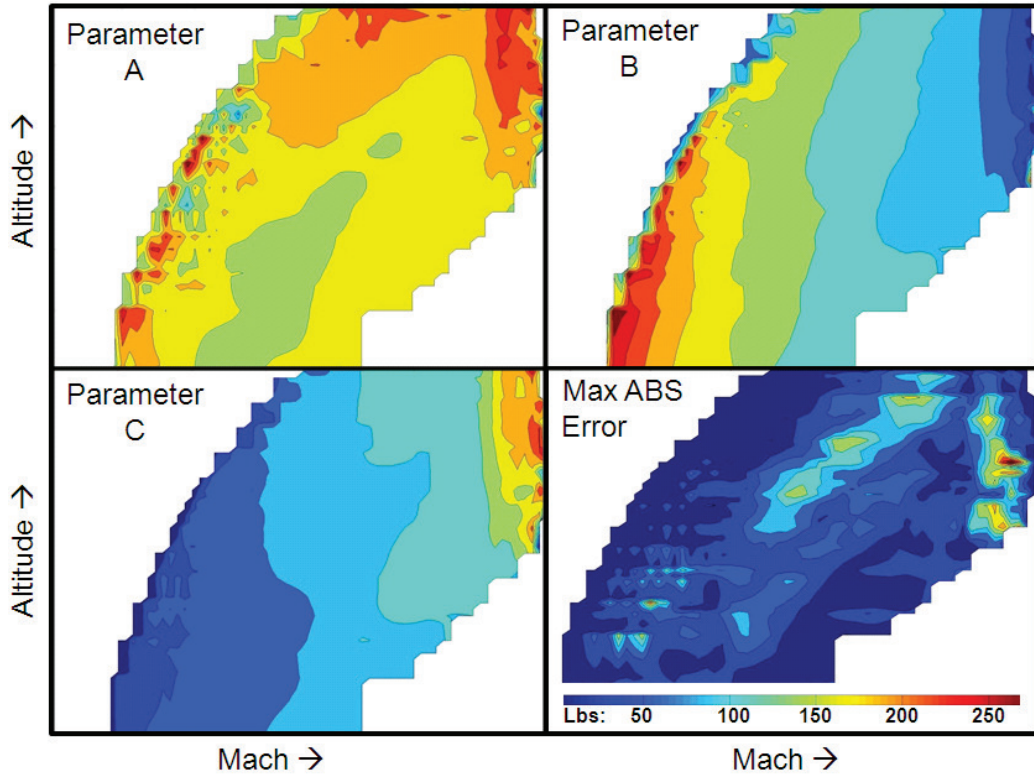


Figure 1.12: An output of the results when the algorithm is modified to find a parameter vector $[\hat{A}\hat{B}\hat{C}\hat{D}]_{zv}$ for each Mach, altitude pair separately.

expression for \dot{W} . Meanwhile the maximum absolute errors in the first model are almost within tolerable limits. Ultimately the decision to use one model over the other will depend on the needs of the end user. If a faster way to compute gross weights over long flight paths is all that is required, then the second model is the better model to use. However, the first model will be easier to use in the construction of optimal flight paths.

1.7 An Optimal Control Formulation of the Tanker Sortie Fuel Planning Problem

The mission to satisfy the aerial refueling requirements generated by the air operations of a single theater of war is referred to as an employment AR mission. The overriding goal of an employment AR mission is to provide every receiver with the

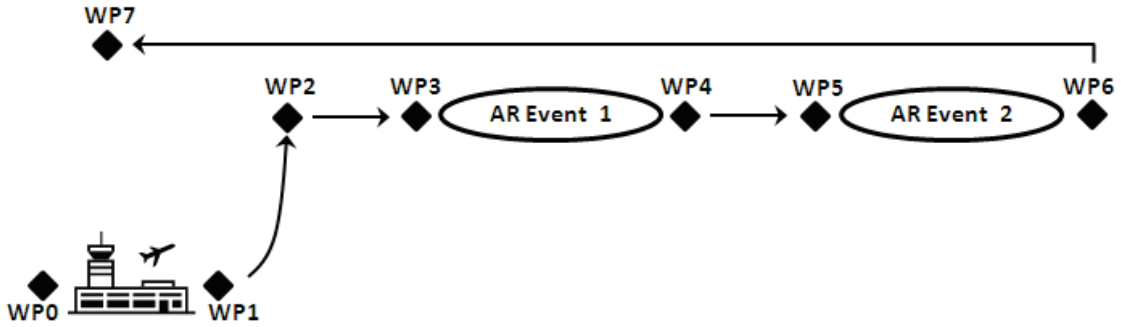


Figure 1.13: Characteristic employment AR mission tanker sortie.

fuel they need, when they need it, where they need it. Consequently the following information is almost always completely specified for an employment AR mission AR event (employment AR event):

- the start time and duration
- the coordinates of the initial and final positions
- the altitude and airspeed of the air refueling maneuver
- the total offload and rate of offload

Thus, given a tanker departure base B_0 , a tanker recovery base B_1 , and a set of employment AR events \mathcal{E} , the Employment Sortie Planning problem (ESP) can be defined as follows:

ESP Find the tanker flight path which departs from B_0 , satisfies the requirements of the AR events in \mathcal{E} , and arrives at a final approach position near B_1 with the required fuel reserve while minimizing a weighted combination of tanker flying time and tanker fuel consumption.

Observe that this problem completely specifies a tanker's state at final approach and many of the conditions the tanker needs to satisfy along the way. Meanwhile, it seems as if finding an optimal departure fuel load is an important part of the problem's solution. This follows from the fact that one of the main goals of this problem is to

minimize total fuel consumption, and the intuitive sense that the fuel flow rate \dot{W} increases with gross weight W under most (if not all) normal flight conditions.

These observations suggest that the problem should be solved backwards. One approach is to divide a sortie into a set of component flight legs and solve the subproblem associated with each flight leg backwards in time and in reverse order. To illustrate this method, consider the following formulations of the subproblems associated with the the example employment AR sortie given in figure 1.13.

1.7.1 Final Cruise Segment

The flight leg between way points 6 and 7 is a model for the final cruise segment of a typical employment tanker sortie. At way point 7 the altitude $Z^{(7)}$, ground speed $V_x^{(7)}$, rate of descent $V_z^{(7)}$, and gross weight $W^{(7)}$ of the tanker are determined by Air Force regulations and characteristics of the recovery base. At way point 6 the altitude $Z^{(6)}$ and airspeed $V^{(6)}$ are determined by the requirements of the AR event. In addition to this, the rate of climb at this way point $V_z^{(6)}$ is assumed to be zero, thus under the no wind assumption, the ground speed $V_x^{(6)}$ should be the same as the airspeed. Finally, the length of the flight leg's ground path $d_{(6,7)}$ is taken to be the great circle distance between the two points. Thus, the problem posed by this flight leg is to find the gross weight $W_*^{(6)}$ at the end of the AR event and the flying time T_* which minimize the given cost function. Using the notation defined in section 1.4, these criteria can be used to formulate the following optimization problem.

$$\begin{aligned}
 \min_{u \in \mathcal{U}} \quad & \int_0^{T_*} C_h dt + C_f W_*^{(6)} \\
 s.t. \quad & \dot{\xi} = F(\xi, u) \\
 & \xi(0) = [W^{(7)}, d_{(6,7)}, Z^{(7)}, V_x^{(7)}, V_z^{(7)}]^T \\
 & \xi(T_*) = [W_*^{(6)}, 0, Z^{(6)}, V_x^{(6)}, 0]^T
 \end{aligned} \tag{1.68}$$

1.7.2 AR Segment

The flight leg between way points 5 and 6 is a model for a typical employment AR event. The first requirement of this segment is that the tanker's final gross weight $W^{(6)}$ must equal the optimizing initial gross weight $W_*^{(6)}$ of the following segment. In addition to this, the altitude Z , airspeed V , and duration T of this flight leg are given by the event's receiver requirements and are assumed to be fixed constant values. Because altitude and airspeed are fixed during this flight leg, it follows that the rate of ascent V_z is zero which implies that the ground speed V_x is equal to the airspeed. Also, it should be observed that during an AR event a tanker's gross weight is affected both by fuel consumption and fuel offload. The most conservative way to model this is to assume that fuel is offloaded in one contiguous time interval at the end of the AR event and to add the constant offload rate R to the rate of fuel flow \dot{W} over that interval. The size of the offload interval τ can be computed by dividing the amount of fuel that needs to be offloaded by the offload rate. Finally, the tanker's boom will likely be down throughout most if not all of an AR flight segment. Therefore, the fuel flow model used in the optimization problem associated with this flight leg, should be parameterized with coefficients estimated from a "Boom Down" specific range data set. Thus, the problem posed by this flight leg is to find the minimum gross weight $W_*^{(5)}$ at the beginning of the AR event needed to satisfy the end of leg fuel requirement and the offload amount while flying at an altitude and airspeed and for a duration of time set by the receiver requirements. Using the notation defined in section 1.4 these criteria can be used to formulate the following optimization problem.

$$\begin{aligned}
 \min \quad & W_*^{(5)} \\
 s.t. \quad & \dot{W}(t) = \begin{cases} -f(W; Z, V_x, 0, 0, 0) + R & t \in [0, \tau) \\ -f(W; Z, V_x, 0, 0, 0) & t \in [\tau, T] \end{cases} \\
 & W(0) = W_*^{(6)} \\
 & W(T) = W_*^{(5)}
 \end{aligned} \tag{1.69}$$

1.7.3 Inter AR Cruise Segment

The flight leg between way points 4 and 5 is a model for any cruise segment between two AR events. The problem posed by this flight leg is almost exactly the same in structure as the one posed by the final cruise flight segment. The distinguishing difference is the fact that the duration of this flight leg is limited to the amount of time that exists between the end of the first AR event and the beginning of the second AR event. The remaining conditions come from the requirements of the two AR events and the fact that the tanker's final gross weight $W^{(5)}$ must equal the optimizing initial gross weight $W_*^{(5)}$ of the following segment. Thus, the problem posed by this flight leg is to find the smallest initial gross weight $W_*^{(4)}$ such that the tanker can depart from the first AR event and arrive on time at the second AR event while satisfying the end of leg fuel requirement. Using the notation defined in section 1.4 these criteria can be used to formulate the following optimization problem.

$$\begin{aligned}
 \min_{u \in \mathcal{U}} \quad & W_*^{(4)} \\
 \text{s.t.} \quad & \dot{\xi} = F(\xi, u) \\
 & \xi(0) = [W_*^{(5)}, d_{(4,5)}, Z^{(5)}, V_x^{(5)}, 0]^T \\
 & \xi(T) = [W_*^{(4)}, 0, Z^{(4)}, V_x^{(4)}, 0]^T
 \end{aligned} \tag{1.70}$$

1.7.4 Initial Cruise Segment

The flight leg between way points 2 and 3 is a model for the initial cruise segment of a typical employment sortie. At way point 3 the tanker's weight is given by the optimizing initial gross weight $W_*^{(3)}$ of the following segment, altitude $Z^{(3)}$ and airspeed $V^{(3)}$ are determined by the requirements of the first AR event, and the rate of climb $V_z^{(3)}$ is assumed to be zero. Under the no wind assumption, this last requirement implies that the tankers ground speed $V_x^{(3)}$ should be the same as the airspeed $V^{(3)}$. Meanwhile, the only component of the tanker's state that is specified at way point 2 is its altitude $Z^{(2)}$ which is required to be the minimum cruising altitude

Z_{\min} allowed by Air Force regulations. Finally the distance $d_{(2,3)}$ between way point 2 and way point 3 is taken to be the great circle distance $d_{(1,3)}$ between way point 1 and way point 3 minus the minimum time climb out distance associated with the tanker's maximum ramp weight. Thus, the problem posed by this flight leg is to find the gross weight $W_*^{(2)}$ and the flying time T_* which minimize the given cost function. Using the notation defined in section 1.4 these criteria can be used to formulate the following optimization problem.

$$\begin{aligned}
\min_{u \in \mathcal{U}} \quad & \int_0^{T_*} C_h dt + C_f W_*^{(2)} \\
s.t. \quad & \dot{\xi} = F(\xi, u) \\
& \xi(0) = [W_*^{(3)}, d_{(2,3)}, Z^{(3)}, V_x^{(3)}, 0]^T \\
& \xi(T_*) = [W_*^{(2)}, 0, Z_{\min}, V_{x*}^{(2)}, V_{z*}^{(2)}]^T
\end{aligned} \tag{1.71}$$

1.7.5 Initial Climb Segment

The flight leg between way points 1 and 2 is a model for the initial climb segment of a typical employment sortie. At way point 2 the tanker's altitude is required to be Z_{\min} as specified by Air Force regulations. In addition to this, the tanker's weight, ground speed, and rate of descent are given by the optimizing initial gross weight $W_*^{(2)}$, the optimizing ground speed $V_{x*}^{(2)}$, and the optimizing rate of descent $V_{z*}^{(2)}$ of the initial cruise segment. Meanwhile, at way point 1, altitude is taken to be 0 ft and airspeed is taken to be $0 \frac{ft}{sec}$. Finally the distance $d_{(1,2)}$ between way point 1 and way point 2 is taken to be the minimum time climb out distance associated with the tanker's maximum ramp weight. Thus, the problem posed by this flight leg is to find the gross weight $W_*^{(1)}$ which minimizes the time T_* it takes to traverse $d_{(1,2)}$, and get to the minimum cruising altitude Z_{\min} . Using the notation defined in section 1.4 these criteria can be used to formulate the following optimization problem.

$$\begin{aligned}
\min_{u \in \mathcal{U}} \quad & \int_0^{T^*} dt \\
s.t. \quad & \dot{\xi} = F(\xi, u) \\
& \xi(0) = [W_*^{(2)}, d_{(1,2)}, Z_{\min}, V_{x^*}^{(2)}, V_{z^*}^{(2)}]^T \\
& \xi(T^*) = [W_*^{(1)}, 0, 0, 0, 0]^T
\end{aligned} \tag{1.72}$$

1.7.6 Example Implementation

Given an employment sortie planning problem with departure base B_0 , a set of N AR events, and a recover base B_1 this method can be implemented using the following algorithm.

1. Get the final approach requirements of B_1
2. Get the receiver requirements of N^{th} AR event
3. Solve the final flight leg problem
4. For $i = 0$ to $(N-1)$
 - Solve the AR Segment problem of AR event $(N-i)$
 - If: there is an AR event $(N-i)-1$
 - Get the receiver requirements of AR event $(N-i)-1$
 - Solve the Inter AR Cruise Segment Problem
 - else:
 - break
- Loop
5. Solve the initial flight leg problem
6. Solve the initial climb problem

One obvious refinement to this algorithm would be the incorporation of a conditional statement at the end of each iteration in the AR event loop which checks to see if the tanker can “get” to the departure base without exceeding its maximum take off weight.

1.8 Suggestions for Future Research

It should be clear that the problems presented in section 1.7 will not be easy to solve considering the governing system developed in section 1.3. Consequently a reasonable next step will be to find ways to either simplify the dynamics of the system, or simplify the tanker sortie planning problem. One immediate simplification would be to assume that each flight leg is flown at a constant altitude. This would cut out the need to consider velocity and acceleration on the Z axis and reduce the number of terms in the dynamics as well as the dimension of optimal control function. It may even be to reasonable remove acceleration along the X axis from the problem and consider optimal control formulations which use velocity along the X axis as the control.

It should also be noted that the problems presented in section 1.7 assume that the best ground path between two points will be the one with the shortest distance. This assumption completely ignores the effects of wind and obstacles created by erupting volcanoes, political boundaries, and anti aircraft weapons. Consequently it will also be useful to find a way to generalize these problems to a sphere which is endowed with a simple but practical wind map and eventually a sphere with both a wind map and no fly zones.

Finally, there are several other characteristic flight planning problems to consider. For example, it would be useful to define maximum orbit offload boundaries given a cruise leg distance, as well as maximum cargo loads given an aircraft, a point of departure, and a point of arrival.

Chapter 2

Tanker Basing Demand Mismatch Index

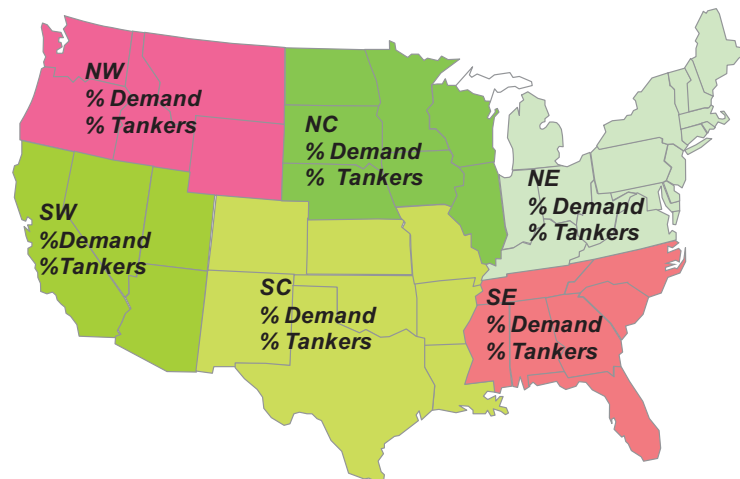


Figure 2.1: Original Six Region Tanker Basing Demand Mismatch Map

2.1 Introduction

In 1992 Headquarters (HQ) Air Mobility Command (AMC) Studies and Analysis was asked to construct a measure that could be used to inform tanker basing decisions made during the first Base Realignment and Closure (BRAC) process. In response to this request they divided the Continental United States (CONUS) into six regions, counted the number of tanker and receiver aircraft within each region, and gave each region a numerical value using the following formula

$$\text{Region Score} = \frac{\% \text{ Share of Receiver Aircraft within Region}}{\% \text{ Share of Tanker Aircraft within Region}} \quad (2.1)$$

This method for quantifying the inter regional balance of the tanker fleet with respect to the geographic distribution of receiver aircraft is known as the Six Region Tanker Basing Demand Mismatch Index (6TBDMI).

The core ideas of the 6TBDMI are: that a region can be given two dimensionless values, one corresponding to its proximity to tanker resources (henceforth a Supply Score or SS) and one corresponding to its proximity to demand for Air Refueling (AR) support (henceforth a Demand Score or DS); that ideally both of these scores would be equal; and that when a region's Supply Score was greater than (less than) its Demand Score, its TBDMI would indicate that tankers needed to be subtracted from (added to) the region. Specifically the 6TBDMI uses a region's percent share of tanker and receiver aircraft as its supply and demand scores. By dividing the demand score by the supply score the 6TBDMI puts the ideal state at a TBDMI value of 1; the oversupply continuum of scores on the half open interval between zero and one; and the under supply continuum of scores on the open set of real numbers greater than one. In addition to this, it is interesting to note that as a region's demand score changes, its 6TBDMI value only changes at a constant rate equal to the reciprocal of its supply score (i.e. $\frac{1}{SS}$). Meanwhile, as a region's supply score changes its 6TBDMI value changes at a rate equal to $(\frac{-DS}{SS^2})$. Thus the 6TBDMI is extremely sensitive to changes in supply score when supply score is small. In particular, as a region's supply score goes to zero, both its 6TBDMI value, and the rate of change in its 6TBDMI value grow without bound. Consequently it would seem as if it is absolutely unacceptable ("Infinitely Bad") for any region to be without a tanker, even regions with demand scores equal to zero. Considering the size of the regions used in the 6TBDMI this amount of sensitivity to supply score would tend to make sense; especially in the light of the fact that it is highly unlikely any of these regions would ever have a zero percent share of receiver aircraft.

Although this scoring method is intuitively clear and provides a good rough estimate of the tanker and receiver aircraft landscape, it is flawed in three critical ways. First, by assigning the same value to every point in a region, the 6TBDMI tacitly assumes that tanker and receiver aircraft are evenly distributed throughout the regions in

Percent of Demand Within a 750 Mile Round Trip Distance

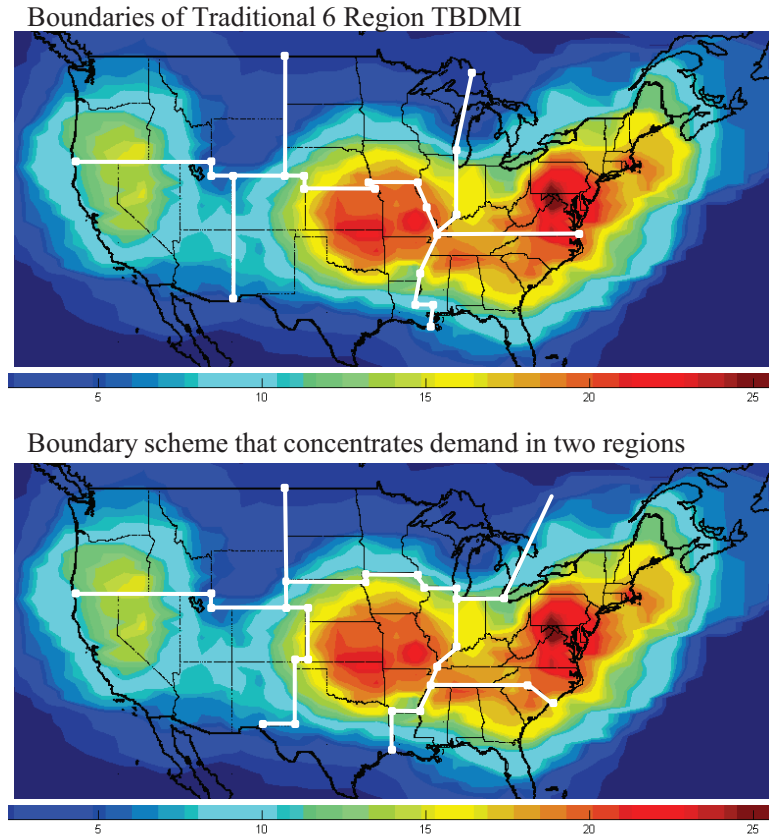


Figure 2.2: The traditional 6 region map, and a boundary scheme that concentrates demand into two regions

which they are located. This is not always true. For example in 2006 there were only two KC-135 tanker bases in the north west region, and both of these bases were in the north west corner of that region. Second, the 6TBDMI assumes that tanker and receiver aircraft only operate within the regions in which they are located. Again this is not supported by the data. For example, Lincoln Nebraska is located just north of the border between the north central and south central regions. Meanwhile, during the period between FY06-Q1 and FY09-Q4, 56% of the round robin tanker sorties flown by the tanker unit at Lincoln Nebraska were flown to support AR events that took place in the south central region. Finally, before the 6TBDMI can be implemented someone needs to decide how the country should be partitioned. This aspect of the index was not clearly defined by its inventors. Consequently present and

future analysts are faced with the decision to either stick with tradition or redraw the boundaries. Complicating this decision is the problem that no matter how the boundary lines are drawn, a discrete regional TBDMI will create winners and losers in what is a politically charged zero sum game. Moreover, because the data do not support the two tacit assumptions discussed above, winners under some regional boundary schemes will likely be losers under others. Consequently the 6TBDMI is politically indefensible. And while this is not a mathematical criteria, it is a very practical thing to consider. Ultimately an index of this nature needs to stand up to intense scrutiny so that it can be used both to shape the best course of action, and defend it.

For these reasons, in December 2009 HQ AMC Analysis, Assessments, and Lessons Learned was asked to repair or replace the 6TBDMI in support of KC-X tanker bed down decisions. The following research was conducted to respond in whole to that request.

2.2 The Ideal TBDMI

The purpose of a TBDMI is to provide decision makers with the ability to clearly see where tankers need to be added and where they can be safely subtracted. This is done by showing them where the demand for AR support is high (low) relative to the supply of neighboring tanker resources, and where it is satisfied (but only just satisfied). Consequently the ideal TBDMI will consider the geographic distribution of the demand for AR support (as opposed to the geographic distribution of receiver aircraft). Moreover, a location's score will depend on all of the AR demand surrounding it as well as all of the tankers in a position to support that AR demand. In addition to this, considering the extremely long range of tanker aircraft, the ideal TBDMI should not produce a set of neighboring locations in which the TBDMI values are starkly different. Specifically, suppose that two locations were said to be equivalent if the difference between their TBDMI values was sufficiently small. Then at any test location on the map it should be possible to find a radius so that every point within the radius of the test point was equivalent to the test point. In short, the ideal TBDMI will be continuous with respect to location. Finally, the results of the ideal

TBDMI will be largely dominated by tanker operations data and parameter values which can be supported by analyses conducted on that data set. This is not to say that the results of the ideal TBDMI won't be subject to decisions made by end users, but rather that end users should only be allowed to insert their judgment when it can be supported by empirical evidence.

2.3 Constructing New Supply and Demand Scores

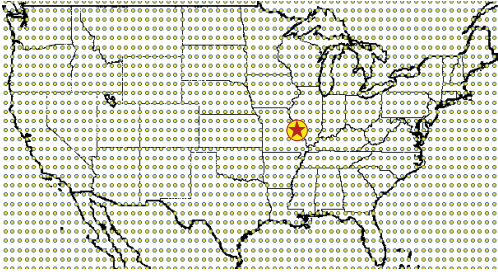


Figure 2.3: A grid of discrete locations generated over CONUS

Consider a location p on the map. Under the 6 TBDMI, p 's supply score is equal to the percent of the tanker fleet located within the same region as p . Thus p 's supply score can be computed with equation (2.2).

$$SS_0(p) = \frac{100 * \sum_{j=1}^J \psi_{(p, TB_j)} T_j}{\sum_{j=1}^J T_j} \quad p \in CONUS \quad (2.2)$$

where T_j is the number of tankers at the j^{th} tanker base, TB_j is the location of the j^{th} tanker base and the function $\psi(p, TB_j)$ is given by equation (2.3).

$$\psi(p, TB) = \begin{cases} 1 & \text{if TB is located in same region as } p \\ 0 & \text{else} \end{cases} \quad (2.3)$$

As discussed in section 2.1, one of the biggest problems with the 6TBDMI is that ψ is a horrible way to determine what should and should not be included in a location's measure of neighboring capacity. First, tanker aircraft are not evenly distributed within regions. Moreover, tankers just beyond a regional boundary are excluded from

a location's supply score no matter how close they are to the location. A better indicator function would include tankers at every tanker base in some symmetric neighborhood around a location p in its supply score. Consider for example the candidate supply score given by equation (2.4).

$$CSS_1(p) = \frac{100 * \sum_{j=1}^J \chi_M(p, TB_j) T_j}{\sum_{j=1}^J T_j} \quad p \in CONUS \quad (2.4)$$

where χ_M is given by equation (2.5).

$$\chi_M(p, TB) = \begin{cases} 1 & \text{if } dist(p, TB) < M \\ 0 & \text{if } dist(p, TB) \geq M \end{cases} \quad (2.5)$$

This function computes the percent share of the tanker fleet within some fixed distance M of a location p . Although it is an improvement on the 6TBDMI supply score, there are still two problems to think about. First χ_M is not continuous with respect to location. Consequently CSS_1 will probably not be continuous either. To see this consider the diagram in figure 2.4.

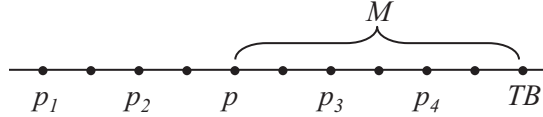


Figure 2.4: Illustrating points of discontinuity generated by a simple indicator function

Because location p is exactly M miles away from tanker base TB , the tankers at TB will not be included in location p 's supply score. Nor will they be included in the supply score of any location to the left of p . Meanwhile these tankers will be included in the supply scores of every point between p and TB . Consequently there will always be points in the neighborhood around p with starkly different supply scores (no matter how small the neighborhood around p is drawn).

Second, this function gives the same weight to every tanker no matter how far it is from a point. To see why this is important, consider two different locations p_1 and

p_2 . Suppose that p_1 is within 300 miles of 2% of the fleet, 600 miles of 6% of the fleet, and 1000 miles of 12% of the fleet. Alternatively suppose that the second location isn't within 700 miles of 1% of the fleet, but is within 1000 miles of 12% of the fleet. The two locations get the same supply score in spite of the fact that p_1 is in an area of the country which is much more densely populated with tankers.

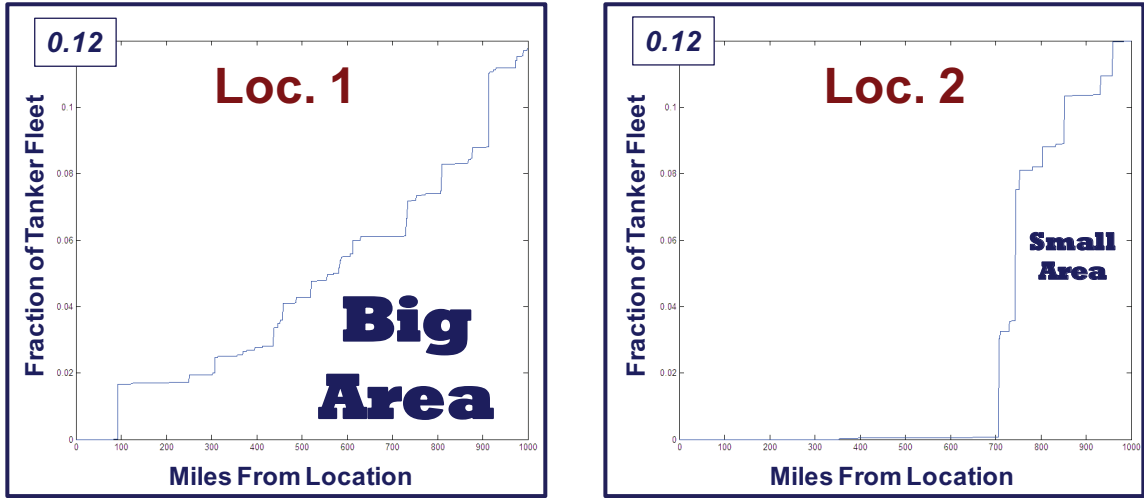


Figure 2.5: The percent share of the tanker fleet within M miles of two example locations

Both of these problems are solved by the candidate supply score given in equation (2.6).

$$CSS_2(p) = \frac{\sum_{j=1}^J \phi_M(p, TB_j) T_j}{\sum_{j=1}^J T_j} \quad p \in CONUS \quad (2.6)$$

where ϕ_M is given by equation (2.7).

$$\phi_m(p, TB) = \begin{cases} M - \text{dist}(p, TB) & \text{if } \text{dist}(p, TB) < M - 1 \\ \frac{(M-1)}{\text{dist}(p, TB)} & \text{if } \text{dist}(p, TB) \geq M - 1 \end{cases} \quad (2.7)$$

This supply score computes the average residual weight given to the tankers around a location. The choice of weighting tankers according to a linear function of distance up to $(M - 1)$ is justified by the fact that tanker sortie costs are approximately linear

with sortie duration [15]. Consequently M should be chosen to reflect factors such as maximum acceptable travel leg length and crew duty day restrictions. Meanwhile, when tankers are positioned beyond $(M - 1)$ miles, the weighting function is designed to decline rapidly from a maximum second tier weight of 1 but never reach zero. Consequently $CSS_2(p)$ will be a continuous function of location, and will always be strictly positive.

The only problem with this function is that it does not produce values that are dimensionless, but rather values in the units of the weighting function. This problem is solved by computing a raw score for every point inside some closed, bounded region of the map, finding the maximum score over that region, and dividing the raw scores by the maximum score.

$$RSS(p) = \sum_{j=1}^J \phi_M(p, TB_j) T_j \quad (2.8)$$

$$MaxRSS = \max_{p \in CONUS} RSS(p) \quad (2.9)$$

$$SS(p) = \frac{RSS(p)}{MaxRSS} \quad (2.10)$$

A location's demand score can be computed in almost exactly the same way. The only slight variation to consider is the fact that AR events often start in one location and end in another. Consequently the weight function needs to be computed using the round trip distance formula given in equation (2.11).

$$RtDist(p, AR) = dist(p, q_1) + dist(p, q_2) \quad (2.11)$$

where q_1 is the starting point of an area of AR activity and q_2 is its end point. Note the distance traveled over the AR legs are excluded from the round trip distance because it is rarely provided by the raw data (for example an AR event could require flying the track multiple times), and because this is a constant length which is independent of the point at which the demand score is being computed.

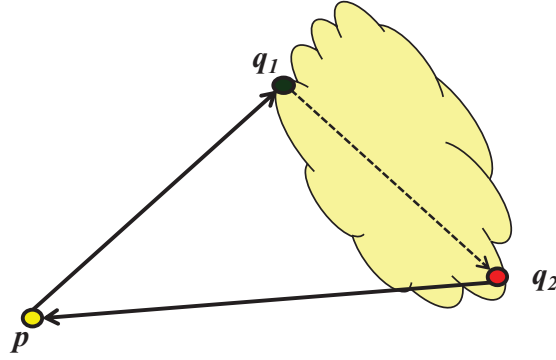


Figure 2.6: Illustration of the round trip distance between a location and an area of AR activity

Thus the formulation for the demand score is given by equations (2.12) through (2.15).

$$\lambda_m(p, AR) = \begin{cases} M - RtDist(p, AR) & \text{if } RtDist(p, AR) < M - 1 \\ \frac{(M-1)}{RtDist(p, AR)} & \text{if } RtDist(p, AR) \geq M - 1 \end{cases} \quad (2.12)$$

$$RDS(p) = \sum_{i=1}^I \lambda_M(p, AR_i) D_i \quad (2.13)$$

$$MaxRDS = \max_{p \in CONUS} RDS(p) \quad (2.14)$$

$$DS(p) = \frac{RDS(p)}{MaxRDS} \quad (2.15)$$

where p is a point in CONUS, AR_i is the i^{th} AR track and D_i is a measure of the demand for AR support observed along the i^{th} track. The list of choices for measuring AR demand includes:

1. Number of round trip tanker Sorties flown to an AR track
2. Hours of tanker time spent at an AR track
3. Pounds of fuel offloaded at an AR track

4. Number of receivers refueled along an AR track

However, the number of round trip (or local) tanker sorties flown to an AR track over a period of time is the only measure of AR demand for which there is reliable data.

2.4 Three Candidate TBDMIs

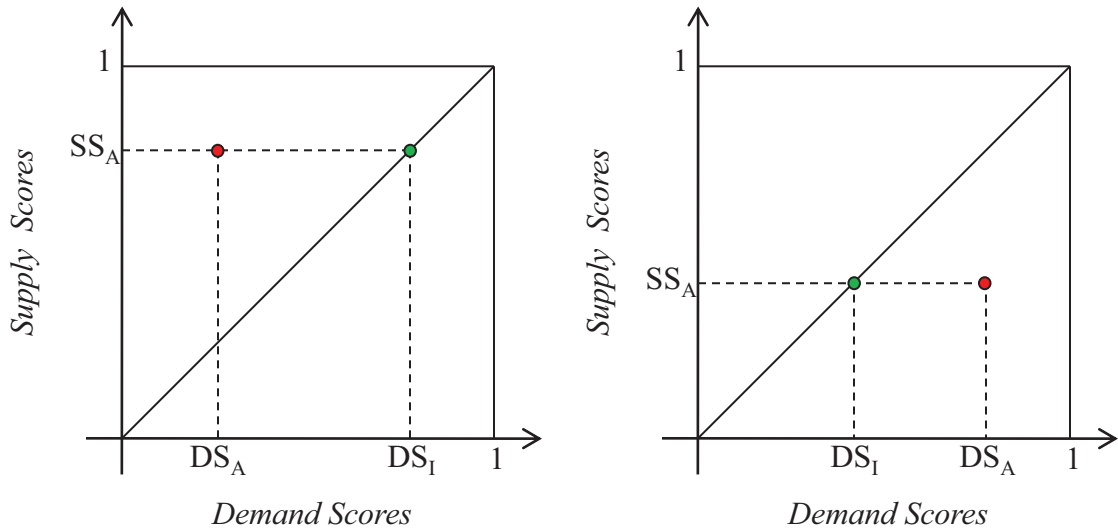


Figure 2.7: Actual Supply Score viewed as the Ideal Demand Score

The supply and demand scores developed in the previous section are intentionally designed to lie on the interval between zero and one. Thus, a location with a demand score near 1 either has a larger percent share of a system's AR demand within its M mile radius, is close to the active AR tracks within its M mile radius, or both. Presumably it would be a good thing if similar statements could be made about the location's proximity to tanker resources, and a bad thing if they could not. Meanwhile a location with a demand score near 0 must have a small percent share of the system's AR demand within its M mile radius, is far from an active AR track, or both. Again it would probably be a good thing if similar statements could be made about such a

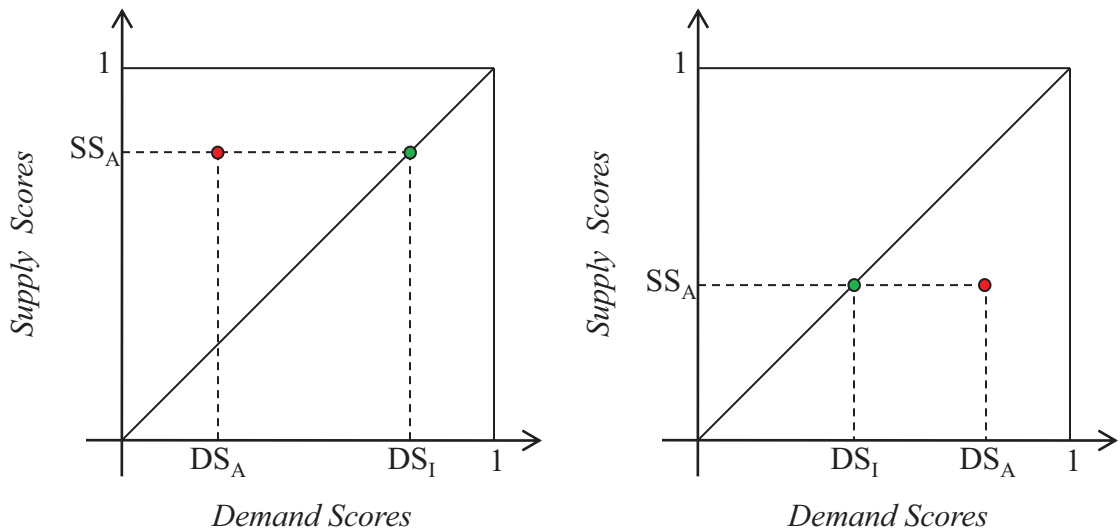


Figure 2.8: Actual Demand Score viewed as the Ideal Supply Score

location's proximity to tanker resources. With that in mind it seems reasonable to assume that the ideal situation is for a location's supply and demand scores to be equal or at least close to equal. Assuming this to be the case, there are two ways to look at a given location's observed or Actual Supply Score(SS_A) and Actual Demand Score (DS_A). On the one hand, a locations SS_A could be viewed as the appropriate level of surrounding AR demand given the actual level of surrounding tanker resources. On the other hand, a location's DS_A could be viewed as the appropriate level of surrounding tanker resources given the active level of surrounding AR demand.

The first point of view might be useful to analysts who are concerned with repositioning receiver aircraft or practice ranges and take the layout of tanker units as a given. Meanwhile the second point of view is useful to analysts who are concerned with adding tankers to the system, or moving tankers around within the system and take the layout of receiver units, practice ranges, and the AR demand signal they generate as a given. Since the second point of view is currently the more relevant of the two, it is the perspective from which three candidate TBDMIs will be evaluated.

First, let p be a location on the CONUS map, and consider the TBDMI obtained by dividing this location's demand score by its supply score.

$$\text{TBDMI}_1(p) = \frac{DS_A(p)}{SS_A(p)} \quad (2.16)$$

This score is the logical descendant of the 6TBDMI score and could be viewed as expressing a location's supply score as a percentage of its actual supply score.

$$\text{TBDMI}_1(p) = \frac{DS_A(p)}{SS_A(p)} = \frac{SS_I(p)}{SS_A(p)} \quad (2.17)$$

Shifting the scale to the left by one unit, as in equation (2.18), generates a second TBDMI that is the same qualitatively, but has a slightly different meaning.

$$\text{TBDMI}_2(p) = \frac{DS_A(p)}{SS_A(p)} - 1 = \frac{SS_I(p) - SS_A(p)}{SS_A(p)} \quad (2.18)$$

Specifically, TBDMI_2 can be viewed as the percent by which a location's SS_A needs to be changed in order for it to have an ideal supply level.

$$SS_A(1 + \text{TBDMI}_2) = SS_A + SS_A\left(\frac{SS_I - SS_A}{SS_A}\right) = SS_I \quad (2.19)$$

The third candidate TBDMI is obtained by removing the denominator from TBDMI_2 .

$$\text{TBDMI}_3(p) = DS_A(p) - SS_A(p) = SS_I(p) - SS_A(p) \quad (2.20)$$

This scoring method can be viewed as computing the absolute difference between a location's observed supply score and its ideal supply score and is qualitatively different from the previous two scoring methods. For example, if a location's demand score increases, its TBDMI_3 value will increase by the same amount. Similarly, if its supply score increases, its TBDMI_3 value will decrease by the same amount. Thus the rate of change in TBDMI_3 is constant in both supply and demand score. This is

radically different from the other two scoring methods in that their rates of change were unbounded on the unit square and depended on either the location’s supply score or both its supply score and demand score. Furthermore, far from being “infinitely bad” for a location to be without any tanker support, the $TBDMI_3$ judges how bad the situation is by the amount of AR demand that is observed in the vicinity of the location. Consequently this index produces a far less dramatic picture, and in some instances a more accurate picture.

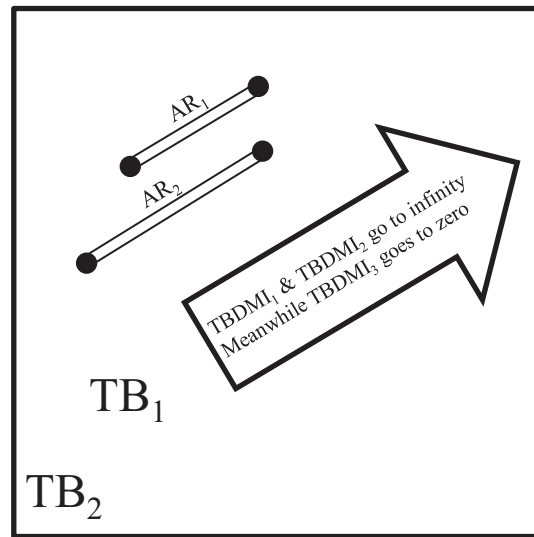


Figure 2.9: A situation where the demand signal will outlast the supply signal

Consider for example locations in an area of the map where both the supply and demand signal are dying out, but the demand signal outlasts the supply signal. In these areas the $TBDMI_1$ and $TBDMI_2$ values will shoot off to infinity meanwhile the $TBDMI_3$ values will rise as the tanker signal weakens, and then steadily fall back to zero when the demand signal finally fades away.

2.5 Residual Concerns and a Fourth TBDMI

Ideally the indices constructed in the previous section would use supply and demand scores which could be easily interpreted as “The Relative Density of Tanker Supply” and “Relative Density of AR Demand” around a location. Although the demand

scores in section 2.3 mute many of the complaints levied against the 6TBDMI, they do not silence all of them and cannot quite be considered in this ideal light. The biggest problem remaining with these scoring methods is that they do not make a distinction between locations around which tankers and or AR demand are evenly distributed and locations around which these structures are distributed asymmetrically.

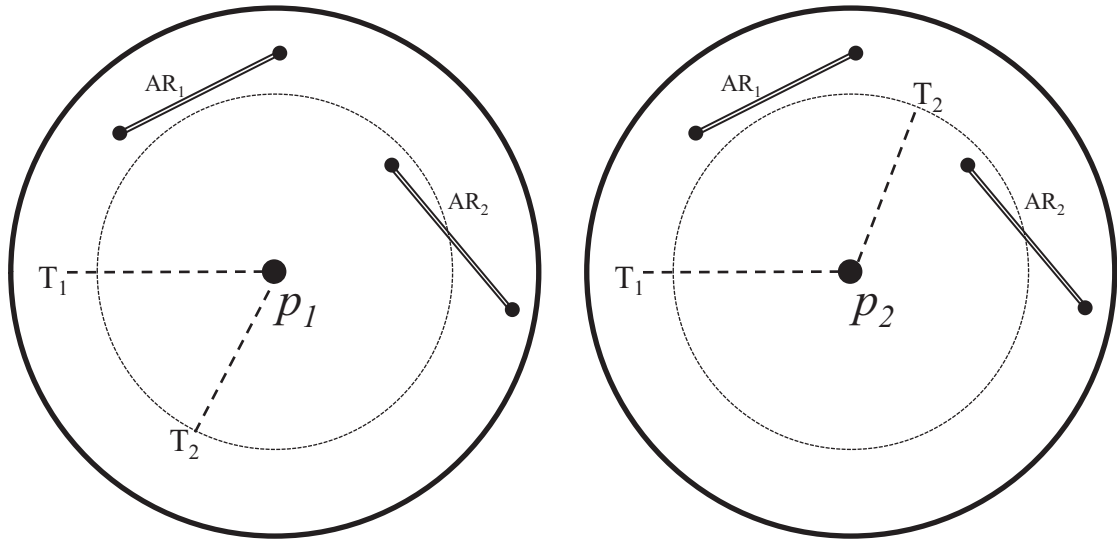


Figure 2.10: Example of two different supply structures with the same supply scores

For example, consider the two locations diagrammed in figure 2.10. The regions around both locations have the same demand structure but two different supply structures. Clearly, location p_2 should have a TBDMI value closer to “ideal” than location p_1 . However, the scores constructed in section 2.3 give both locations the same supply score and thus the same TBDMI values. The difference between the new scoring methods and the 6TBDMI is that every location is evaluated independently of every other location. Consequently locations to the right of p_1 will have smaller and smaller supply scores, and thus larger and larger TBDMI values. Meanwhile locations to the right of location p_2 will not see their supply scores drop off as quickly.

Another lesser problem is that tankers beyond a location’s M mile radius may have extremely little influence on its supply score, even though these tankers might have a great deal of influence on the level of support provided to AR tracks located within its M mile radius. Again the fact that every location is evaluated independently of every other location, and the fact that the supply and demand scores are constructed

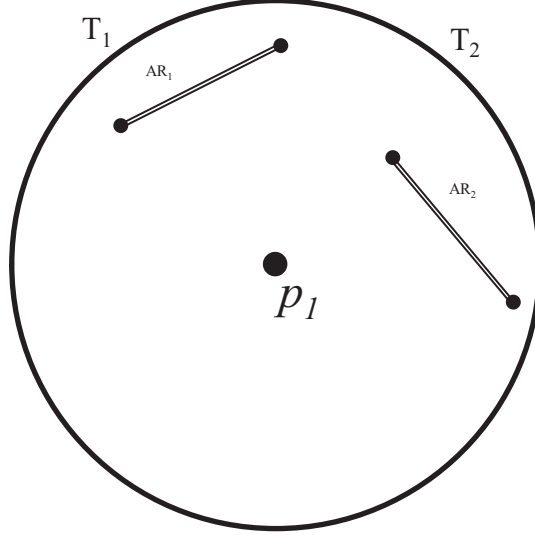


Figure 2.11: Example of tankers located just outside a locations M mile radius

to be continuous with respect to location means that points above p_1 will see their supply scores steadily increase along with their demand scores.

That being said, there is enough residual concern to motivate the development of a fourth candidate TBDMI. TBDMI₄ looks at a location as if it could be the center point of a brand new tanker base and asks the question: “To what extent would phantom tankers positioned at this location benefit its surrounding demand for AR support?”. To answer this question for a given location, CTBMI₄ supposes that the location is the bed down location of a phantom squadron of K tankers. It then computes the percentage that these K tankers represent to each of the neighboring AR tracks adjacent supply of tankers. Finally, it uses these percentages to weight each track’s demand for AR support. The benefit of adding the phantom tankers at the location is then judged by the sum of the weighted demand signals. A rigorous formulation of this scoring method is formulated in equations (2.21) through (2.24).

$$DW_i(p) = \frac{K\lambda(p, AR_i)}{K\lambda(p, AR_i) + \sum_{j=1}^J T_j\lambda(TB_j, AR_i)} \quad (2.21)$$

$$RS(p) = \sum_{i=1}^I DW_i(p)D_i \quad (2.22)$$

$$MaxRS = \max_{p \in CONUS} RS(p) \quad (2.23)$$

$$TBDMI_4(p) = \frac{RS(p)}{MaxRS} \quad (2.24)$$

where p is a location in CONUS, λ is the distance weighting function defined in equation (2.12) and K is the number of phantom tankers temporarily bed down at each location.

The advantage of this index over the previous indices is that it evaluates the relationship between tankers and AR tracks by the distance between the tankers and the tracks rather than boldly assuming that tankers are uniformly distributed around a given location. The disadvantage of using this index is that analysts will have to choose and defend the value of a second parameter. In addition to this, the meaning of a location's index value is much less clear. In the very least it ranks the locations with respect to the benefit of adding tankers. However, *the true value of this index is its ability to validate or contradict the results generated by the previous three indices.*

2.6 Results

The following results are based on actual tanker operations data taken from the FY06-Q1 through FY09-Q4 time period. It is believed that the geographic distribution of AR demand over the next five to ten years will closely resemble the geographic distribution of demand over the last four years. Consequently, to determine the location of the first KC-X squadrons, this data has been paired with the post BRAC FY12 tanker basing plan.

First, consider the results obtained from the 6TBDMI (see figure 2.12). These results were generated by dividing a region's percent share of AR events by its percent share of tankers because the receiver bed down plan is not currently available for analysis. The regional values produced by this TBDMI indicate that the North East and South Central regions have more tankers than they should given their levels of AR demand,

Six Region, Supply, Demand*, and TBDMI Scores

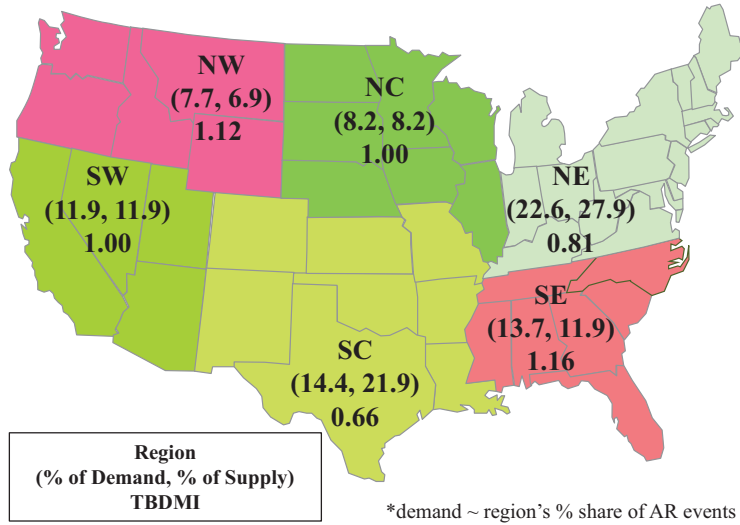


Figure 2.12: Results of the 6TBDMI

the North Central and South West regions have the correct number of tankers given the share of demand observed within their borders, and that the North West and South East regions need more tankers. However, because these regions are so big, further analysis would be needed to determine where in the North East and South Central regions tanker aircraft can be safely removed, and where in the North West and South East they should be added.

Now consider the maps drawn using the new TBDMIs with $M = 500$ and $M = 700$. These maps demonstrate that there isn't a general need for tankers all over the North West or all over the South East. On the contrary, all four of the new TBDMIs indicate that if tankers are needed anywhere near the North West, they are really only needed along the border between California and Oregon. Moreover, features observed on these maps indicate that the 6TBDMI may erroneously support the conclusion that the entire South West region is adequately supported.

A slightly more confusing story develops over the South East Region. Consider the demand score map generated for $M = 500$ (top right corner of figure 2.13). This map reveals a corridor of demand that stretches from north west Florida, through eastern Georgia, and into South Carolina. Although this corridor becomes less and less apparent in the demand score maps as M increases, it continues to show up in

all four of the new TBDMI maps through $M = 750$ and in the fourth TBDMI map through $M = 1000$. This suggests that if tankers are needed in the South East, then they should be located somewhere along this corridor.

As regards regions with too many tankers, all of the new TBDMIs support the conclusion that tankers based in Michigan, Wisconsin, and Indiana are out of position. However, they also support the addition of tankers somewhere along the Atlantic coast between Virginia and Maine. Meanwhile, considering the size and strength of the demand signal over Kansas and Missouri, even at $M = 500$, it is unlikely that any of the tankers currently located at bases in the South Central region should be removed.

On a final note, consider the $M = 500$ and $M = 700$ maps, and observe the demand signal over Arizona and the demand signal off the north east tip of Maine pushing toward Nova Scotia. These signals have about the same intensity and exist in regions that are not significantly different in terms of surrounding tanker capacity. However, they behave quite differently. The area off the coast of Maine generates TBDMI_1 and TBDMI_4 scores which explode partly because the track off of the East Coast is oriented in such a way that its demand signal outlasts the supply signals of the tankers to the south west and partly because there are so few tankers in the area. Meanwhile the demand over Arizona is surrounded on four sides by tanker bases. Consequently the TBDMI_1 and TBDMI_4 values get large, but don't explode. In contrast the TBDMI_3 maps show that the absolute difference between supply and demand scores is about the same all along the east coast.

2.7 Going Forward (Final Caveats)

It is important to note that the TBDMIs developed above do not compute or consider the minimum or maximum number of tankers needed to support a given level of AR demand. Consequently they do not indicate in an absolute sense whether an area needs more tankers or whether it is in a position to relinquish a few tankers. They can only indicate in a relative sense if a location has more tankers than other areas, or fewer tankers than other areas, and if this surplus or deficit can be justified given the location's relative level of AR demand. This should not be a problem when the

M = 500

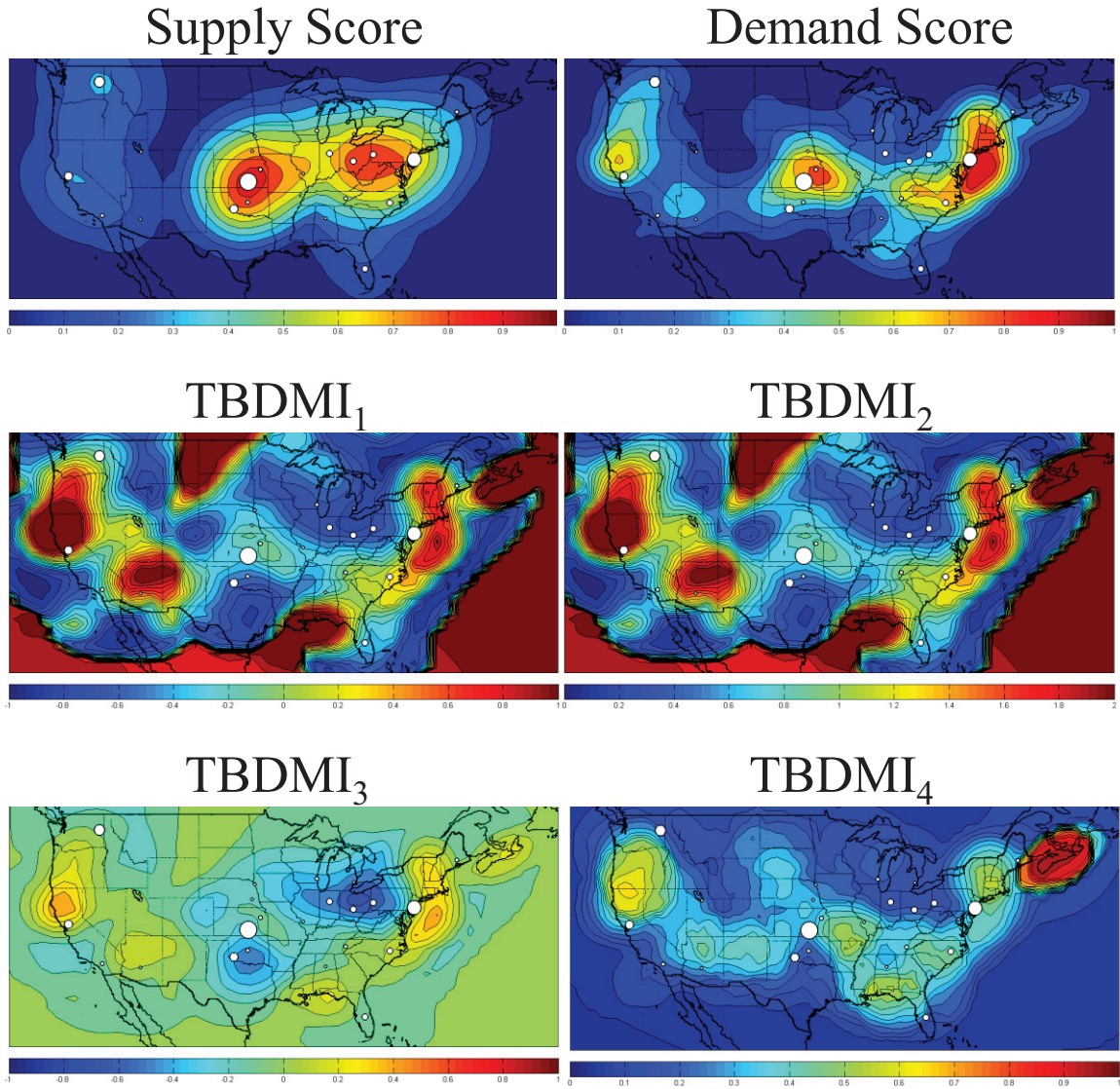


Figure 2.13: Results of the new TBDMIs for $M = 500$

M = 750

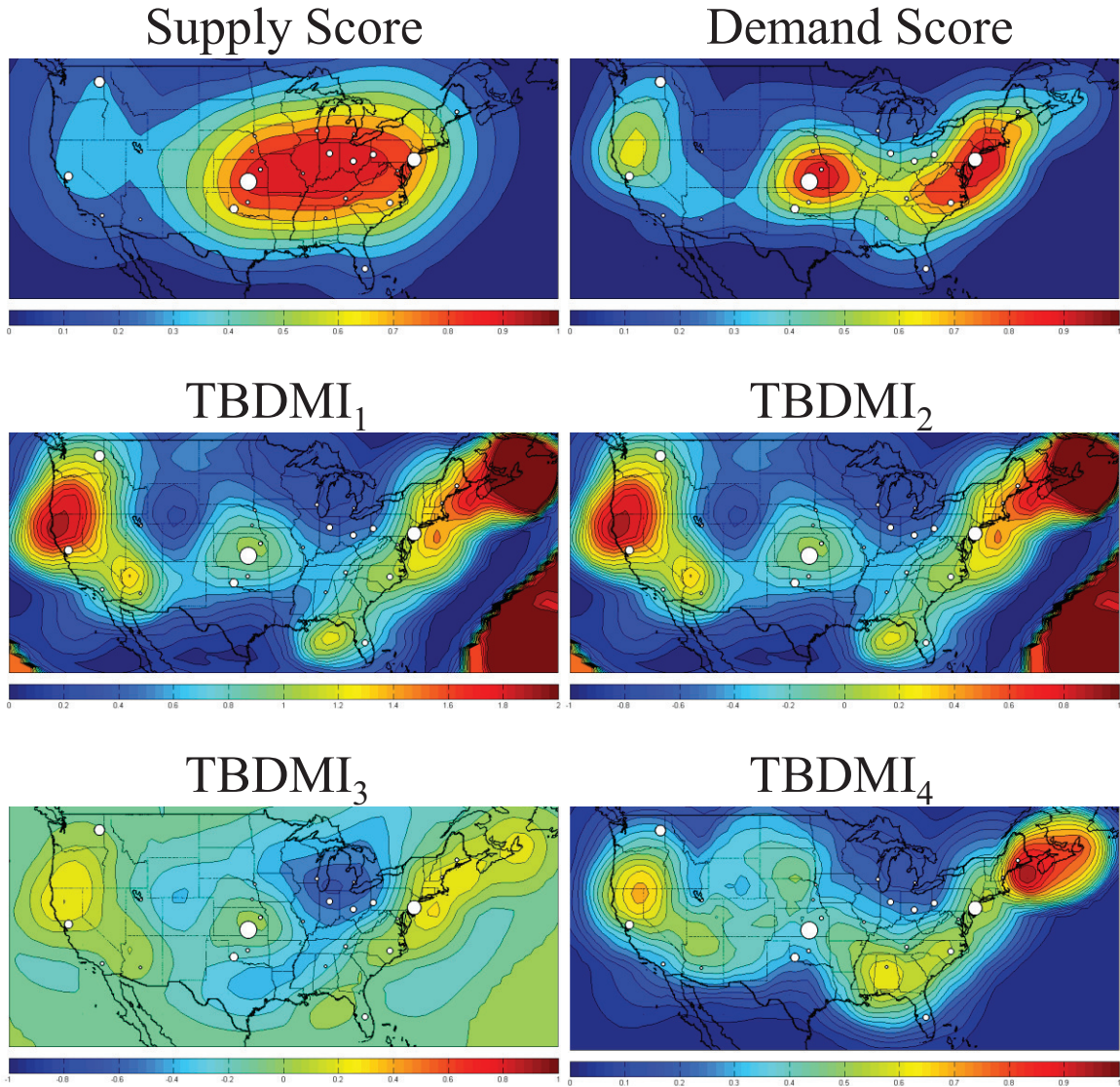


Figure 2.14: Results of the new TBDMIs for $M = 750$

M = 1000

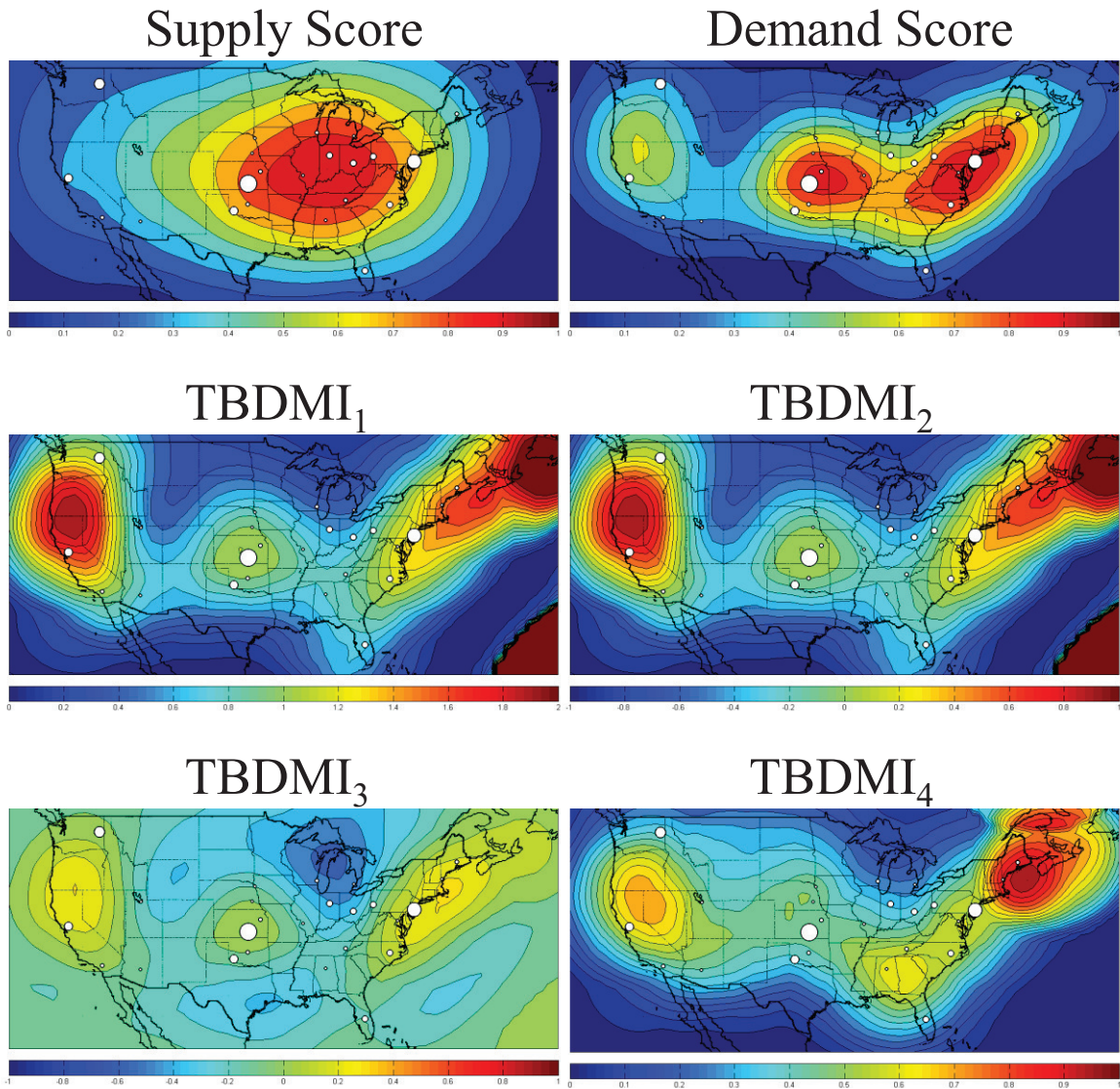


Figure 2.15: Results of the new TBDMIs for $M = 1000$

M = 1250

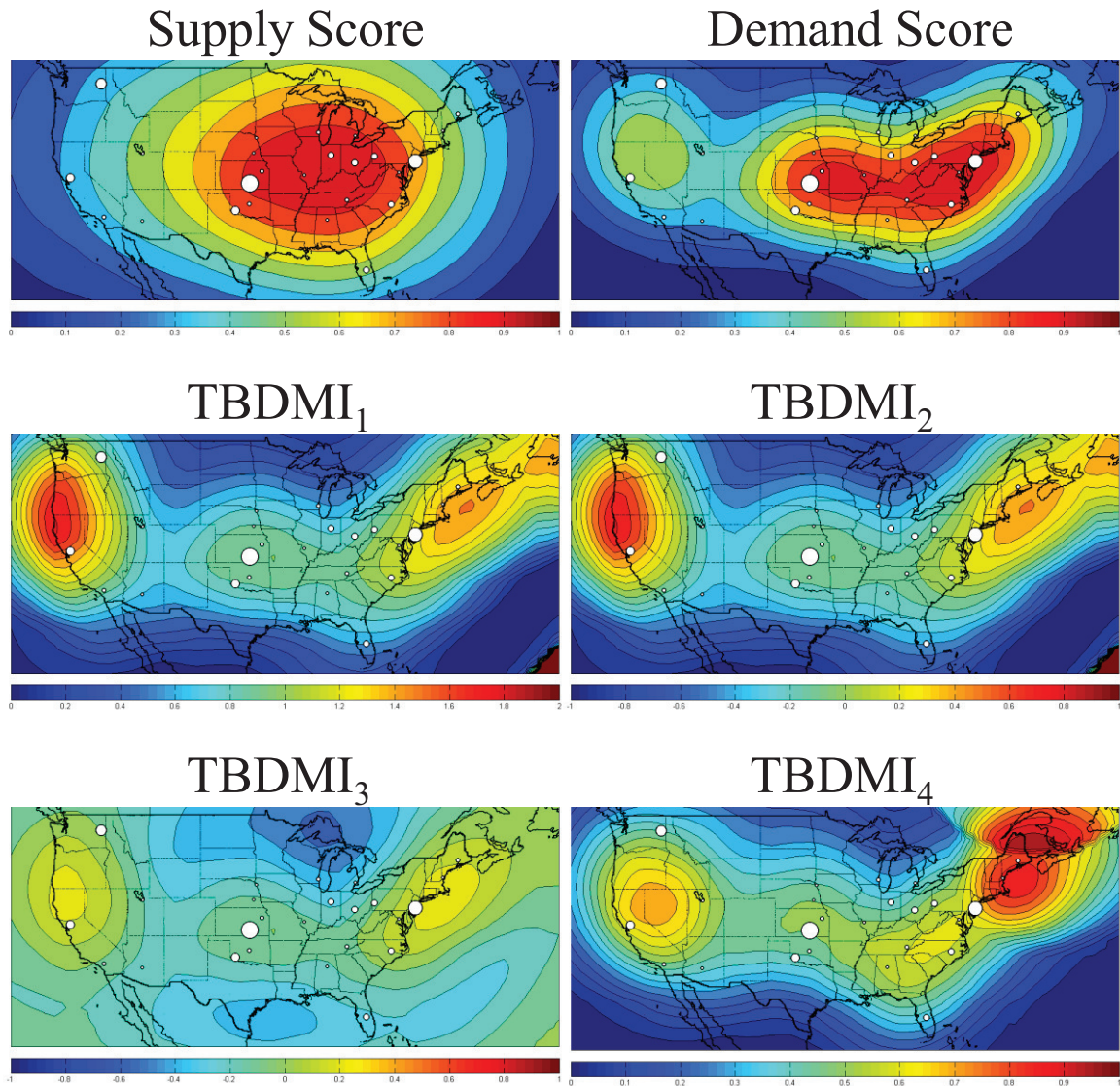


Figure 2.16: Results of the new TBDMIs for $M = 1250$

supply of tankers is less than or equal to the supply of tankers needed to satisfy AR demand because the goal in this situation is to spread the resources as evenly as possible. However, when there are more tankers than are needed to satisfy the system's demand, these TBDMIs could suggest that areas with an ample supply of tankers need yet more tankers. This would happen if, for example, an area had a relatively small surplus compared to other areas, but contained a relatively large share of the total demand for AR support. Consequently further research is needed to find ways to include minimum and maximum tanker supply requirements into the TBDMIs.

In addition to this it is also necessary to look more deeply into how TBDMIs should be used to find the optimal tanker basing strategy. Currently the Air Force is using the TBDMI and several other factors to simply rank candidate tanker bases and is only choosing from among the top ranked bases. While this may be a reasonable approach to choose the next tanker base, or perhaps the next two tanker bases, this is probably not a good way to generate the best network of tanker bases. Ultimately long term strategic tanker basing decisions should be considered in the framework of a location routing problem which takes both construction and operating costs into consideration. Ultimately TBDMIs could be used to find initial solutions to location routing problems designed to find optimal tanker basing strategies. They could also be used to evaluate, or at least spot check the results generated by problem solving algorithms.

Chapter 3

Using TBDMIs In Tanker Basing Analysis

3.1 Introduction

Generating maps that compare a single basing structure to current or forecast operations data, as was done in section 2.6, is an obvious and important use of the TBDMIs. Their real value, however, may be their ability to help decision makers choose new basing structures. Specifically, TBDMIs can be used to evaluate the wisdom of implementing tanker basing strategies generated by solving optimal location routing problems. Tractable forms of these problems attempt to capture the numerous details of day to day tanker operations with a single objective value and a minimal set of constraints. Consequently it is unlikely that assertions such as “An acceptable duality gap has been achieved” and “All integral constraints are satisfied” will resonate with decision makers who are thoroughly versed in the complexities of tanker operations and are often skeptical of oversimplified scheduling models. Constructs, such as the TBDMIs, provide an independent and easily understood framework which can be used to study the interaction between a given bed down plan and anticipated demand for AR support. Furthermore, because the maps produced by these indices clearly illustrate the the strengths and weaknesses of a particular basing strategy, TBDMIs provide decision makers yet another way to compare and possibly decide between different basing strategies.

This use of the TBDMIs is illustrated in two slightly different ways. First, the proposed FY12 basing strategy is compared to the results generated by a reasonably

simple location routing problem. After that, an optimal basing strategy generated by evaluating the complete data set, is compared to an optimal basing strategy generated by only evaluating low priority AR events.

3.2 Location Routing and Scheduling Models

The basing strategies discussed in the following sections are obtained by evaluating actual tanker operations data with the optimization problem given by equations (3.1) through (3.9).

$$\min \sum_{k=1}^K \sum_{l=1}^L X_{kl} D_{kl} \quad (3.1)$$

such that:

$$1 = \sum_{l=1}^L X_{kl} \quad 1 \leq k \leq K \quad (3.2)$$

$$\text{EPD}_S * S_l \geq \sum_{k \in D_h} X_{kl} \quad 1 \leq l \leq L, 1 \leq h \leq H \quad (3.3)$$

$$\text{EPW}_S * S_l \geq \sum_{k \in W_i} X_{kl} \quad 1 \leq l \leq L, 1 \leq i \leq I \quad (3.4)$$

$$\text{EPM}_S * S_l \geq \sum_{k \in M_j} X_{kl} \quad 1 \leq l \leq L, 1 \leq j \leq J \quad (3.5)$$

$$\text{MS} \geq \sum_{l=1}^L S_l \quad (3.6)$$

$$\text{MSPB} \geq S_l \quad 1 \leq l \leq L \quad (3.7)$$

$$X_{kl} \quad \text{Binary} \quad (3.8)$$

$$S_l \quad \text{Integer} \quad (3.9)$$

The indices $h, i, j, k,$ and l refer to day, week, month, AR event, and tanker Base IDs, respectively. The binary decision variable X_{kl} is equal to 1 if event k is assigned to base l and the integer decision variable S_l defines the number of squadrons positioned at base l .

The constraints defined in equation (3.2) require that each AR event is assigned to exactly one tanker base. Meanwhile the constraints defined by equations (3.3) through (3.5) control the number of AR events given to each base per day, week, and month of the time horizon. Note that the sums in the second collection of constraints are restricted to events k that occurred on the h^{th} day ($k \in D_h$), in the i^{th} week ($k \in W_i$), or during the j^{th} month ($k \in M_j$). Also note that the constants EPD_S , EPW_S , and EPM_S dictate the number of events per squadron per day, week, and month respectively, and do not distinguish between Active Duty, Air Force Reserve, or Air National Guard squadrons. Together the collection of constraints generated by equations (3.2) through (3.5) tacitly assume that each tanker sortie will only support one AR event. This assumption is largely supported by the data. Specifically, during the period between FY06-Q1 and FY09-Q4, 90% of all CONUS AR events were supported by a round robin tanker sortie and 90% of all round robin tanker sorties only supported one AR event.

The constraints defined in equation (3.6) and (3.7) use the constants MS (maximum number of squadrons) and MSPB (maximum number of squadrons per base) to limit the number of squadrons put into service and the number of squadrons allowed at each base. In all of the results given in the following sections it is assumed that 32 squadrons of 12 tankers per squadron will be put into service, and that no more than 3 squadrons will be positioned at each base. It is important to realize that the observed data and a choice of maximum number of squadrons define minimum allowable values on the constants EPD_S , EPW_S , and EPM_S . For example, the problem is infeasible if the product $(EPD_S)(MS)$ is less than the observed maximum number of events on any of the days defined in the data set. In the results given below, EPD_S , EPW_S , and EPM_S are set at 4, 14, and 56 respectively.

The objective function of this model uses the distance D_{kl} between the k^{th} event and the l^{th} tanker base to compute the total distance flown to support all of the AR events in the data set. Minimizing this objective function should drive the model toward a basing strategy which has the potential to fly the least number of miles while satisfying all of the scheduling constraints.

Finally, a pure scheduling model is employed to find schedules with the absolute minimum distance traveled while satisfying a similar set of constraints. This model is given in equations (3.10) through (3.15).

$$\min \sum_{k=1}^K \sum_{l=1}^L X_{kl} D_{kl} \quad (3.10)$$

Such That:

$$1 = \sum_{l=1}^L X_{kl} \quad 1 \leq k \leq K \quad (3.11)$$

$$\text{EPD}_T * T_l \geq \sum_{k \in D_h} X_{kl} \quad 1 \leq l \leq L, 1 \leq h \leq H \quad (3.12)$$

$$\text{EPW}_T * T_l \geq \sum_{k \in W_i} X_{kl} \quad 1 \leq l \leq L, 1 \leq i \leq I \quad (3.13)$$

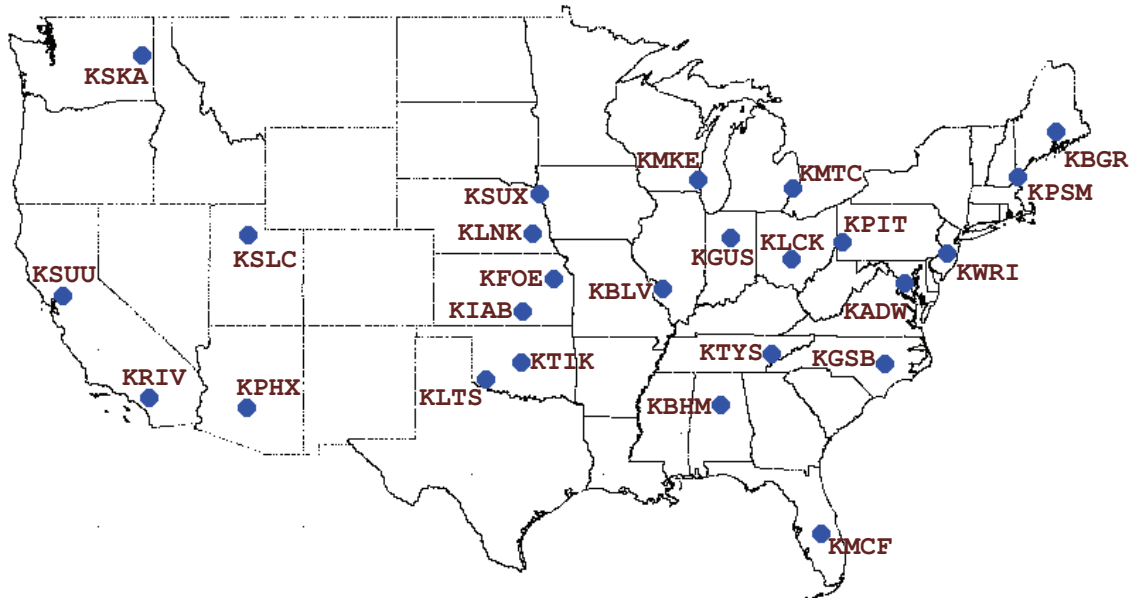
$$\text{EPM}_T * T_l \geq \sum_{k \in M_j} X_{kl} \quad 1 \leq l \leq L, 1 \leq j \leq J \quad (3.14)$$

$$X_{kl} \quad \text{Binary} \quad (3.15)$$

The main difference between this model and the previous one is that it uses tankers as the smallest divisible unit instead of squadrons. This is done so that the scheduling model can evaluate both the bed down plans generated by the previous model, which use 384 tankers divided into 32 squadrons of 12 tankers, and the FY12 basing plan, which uses 388 tankers divided into squadrons of varying size. In order to accommodate this change, the scheduling model uses the constants EPD_T , EPW_T , and EPM_T to control the number of events assigned to each tanker base per tanker per day, week, and month respectively. Finally to maintain a correspondence with the previous model, the results given below were generated with these values set at 4/12, 14/12, and 56/12 respectively.

3.3 Tanker Basing

The Location Routing model defined in the previous section was given the set of 25 tanker bases found in the FY12 tanker basing plan (see figure 3.1), and was used



ICAO Base Name	ICAO Base Name	ICAO Base Name	ICAO Base Name	ICAO Base Name
KADW Andrews	KGSB Seymour Johnson	KLTS Altus	KPIT Pittsburgh	KSUU Travis
KBGR Bangor	KGUS Grissom Field	KMCF MacDill	KPSM Pease	KSUX Souix City
KBHM Birmingham	KIAB McConnell	KMKE Mitchell Field	KRIV March	KTIK Tinker
KBLV Scott	KLCK Rickenbacker	KMTC Selfridge	KSKA Fairchild	KTYS McGhee Tyson
KFOE Forbes Field	KLNK Lincoln	KPHX Phoenix	KSLC Salt Lake City	KWRI McGuire

Figure 3.1: Air fields at which the FY12 tanker basing plan locates tanker aircraft

to evaluate tanker operations data from three different time periods: FY06-FY07, FY07-FY08, and FY08-FY09. A model run of the entire period was not evaluated because the laptop, on which this work was done, did not have enough memory to support a model run of that size.

The results generated by the model were largely the same for all three time periods. Of the 25 bases, 15 were given the same number of tankers across the entire data set. More importantly 3 distinct regions were given the same exact resource structure. Specifically, the set of 96 tankers allocated to the western states was always divided so that Fairchild AFB (KSKA) got 24, Salt Lake City (KSLC) got 12, Travis AFB (KSUU) got 36, and Phoenix (KPHX) got 12. The set of 72 tankers positioned along the mid Atlantic down through Florida was always divided so that there were 24 at McGuire (KWRI), 8 at Andrews (KADW), 24 at Seymour-Johnson (KGSB), and 12 at Mac Dill (KMCF). And the set of 36 tankers allocated to the region between western Nebraska and eastern Wisconsin was always divided evenly between Lincoln Nebraska (KLNK), Sioux City Iowa (KSUX), and General Mitchell Field (KMKE).

ICAO	FY0607	FY0708	FY0809
KADW	12	12	12
KBGR	36	36	24
KBHM	12	12	24
KBLV	12	24	24
KFOE	24	12	12
KGSB	24	24	24
KGUS	12	0	12
KIAB	12	24	12
KLCK	0	12	0
KLNK	12	12	12
KLTS	24	12	12
KMCF	12	12	12
KMKE	12	12	12
KMTC	0	0	0
KPHX	12	12	12
KPIT	12	0	12
KPSM	12	24	24
KRIV	12	12	12
KSKA	24	24	24
KSLC	12	12	12
KSUU	36	36	36
KSUX	12	12	12
KTIK	12	12	12
KTYS	12	12	12
KWRI	24	24	24

Figure 3.2: Basing plans generated by the Location Routing Model

The differences between the three optimal basing strategies are easily explained by looking at the $M = 500$ and $M = 750$ demand score maps of the three periods (figures 3.3 and 3.4 respectively). These maps clearly show that, in relative terms, the eastern edge of the south west and the region off the north east tip of Maine saw less activity with the progression of time while the south east and western Virginia saw their relative share of AR demand increase. As a result, the model positioned progressively fewer tankers in Oklahoma and Kansas, and progressively more tankers at bases which are closer to the south east and the Ohio River valley.

The scheduling model was used to evaluate each basing strategy for the FY06-FY07 and FY08-FY09 time periods separately, and in each of the eight cases it was able to

M=500 Demand Score Maps

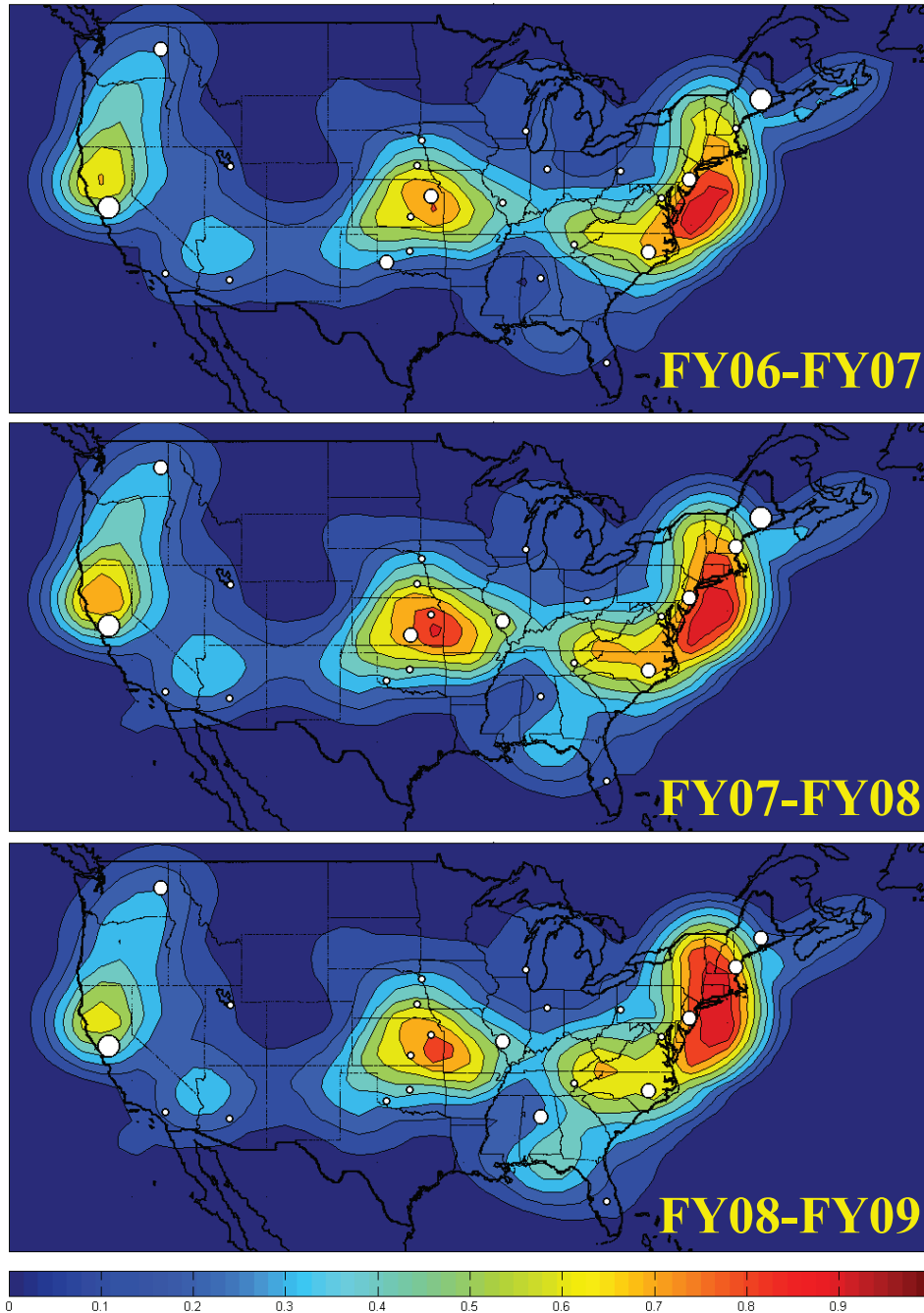


Figure 3.3: M=500 Demand Score Maps for the three different time periods

M=750 Demand Score Maps

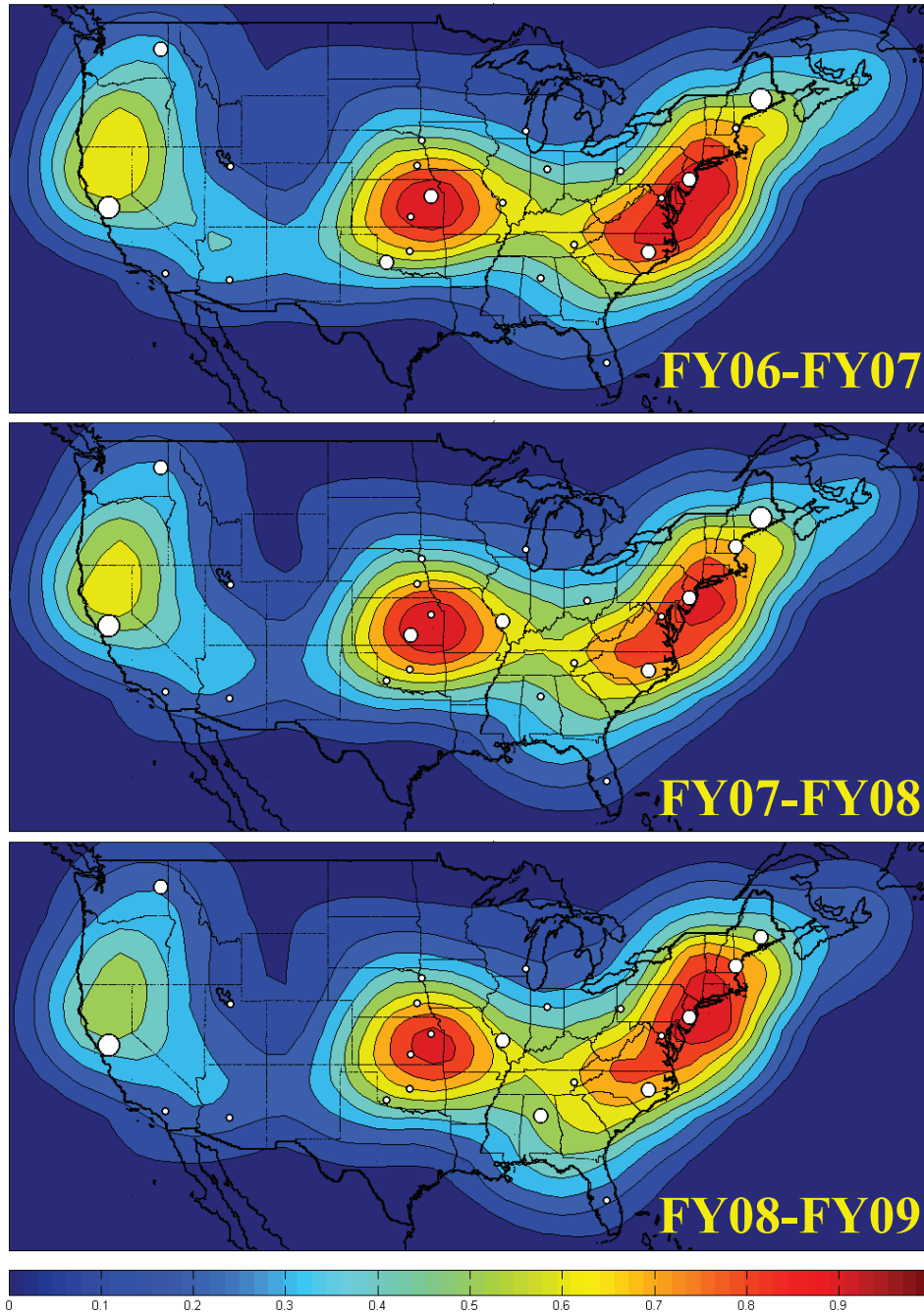


Figure 3.4: M=750 Demand Score Maps for the three different time periods

find an optimal solution. The results generated by these model runs are presented in figure 3.5.

Basing Strategy	FY06-FY07	FY08-FY09	Totals
FY12	15,300,838	13,809,288	29,110,126
Opt 0607	13,212,094	12,532,664	25,744,758
Opt 0708	13,143,756	12,386,439	25,530,195
Opt 0809	13,367,530	12,333,754	25,701,284

Figure 3.5: Results from optimal scheduling model

The Opt 0708 basing strategy produced the best schedules from among the three optimal basing strategies. Considering the fact that this basing plan was generated from half of the FY06-FY07 period and half of the FY08-FY09 period, and the fact that both periods have about the same volume of AR activity, this result tracks with expectations. That being said, there is a less than 1% difference between the distances traveled under these three basing plans and this difference only represents about 63,825 miles per year. In light of the distances traveled per tanker sortie a difference that small can be attributed to the optimal scheduling model finding better matches for about 100 to 200 AR events per year under the Opt 0708 basing plan. In a similar analysis, the FY12 basing plan generated schedules which flew an additional 894,982 miles per year. This can be attributed to the optimal scheduling model finding about 1,800 better assignment per year with the Opt 0708 base plan. Although that seems like a large number, it only accounts for 10% of the annual demand for AR support. Consequently, after accounting for the simplifying assumptions used to make the models tractable, it might be reasonable to brush the difference between the FY12 and Opt 0708 basing aside. However, when the 14% difference in distance flown is viewed alongside the TBDMI maps generated by the Opt 0708 and FY12 basing strategies (figures 3.6 and 3.7 respectively), the argument for the Opt 0708 basing strategy is much more compelling.

The TBDMI₁ maps clearly show that the Opt 0708 tanker basing strategy does a better job of distributing tanker resources with respect to the geographic distribution of AR demand. In particular, it shows that little to no damage is done by reallocating some of the tankers currently positioned in the central corridor, and almost no

TBDMI₁ Scores for OPT 0708 Basing

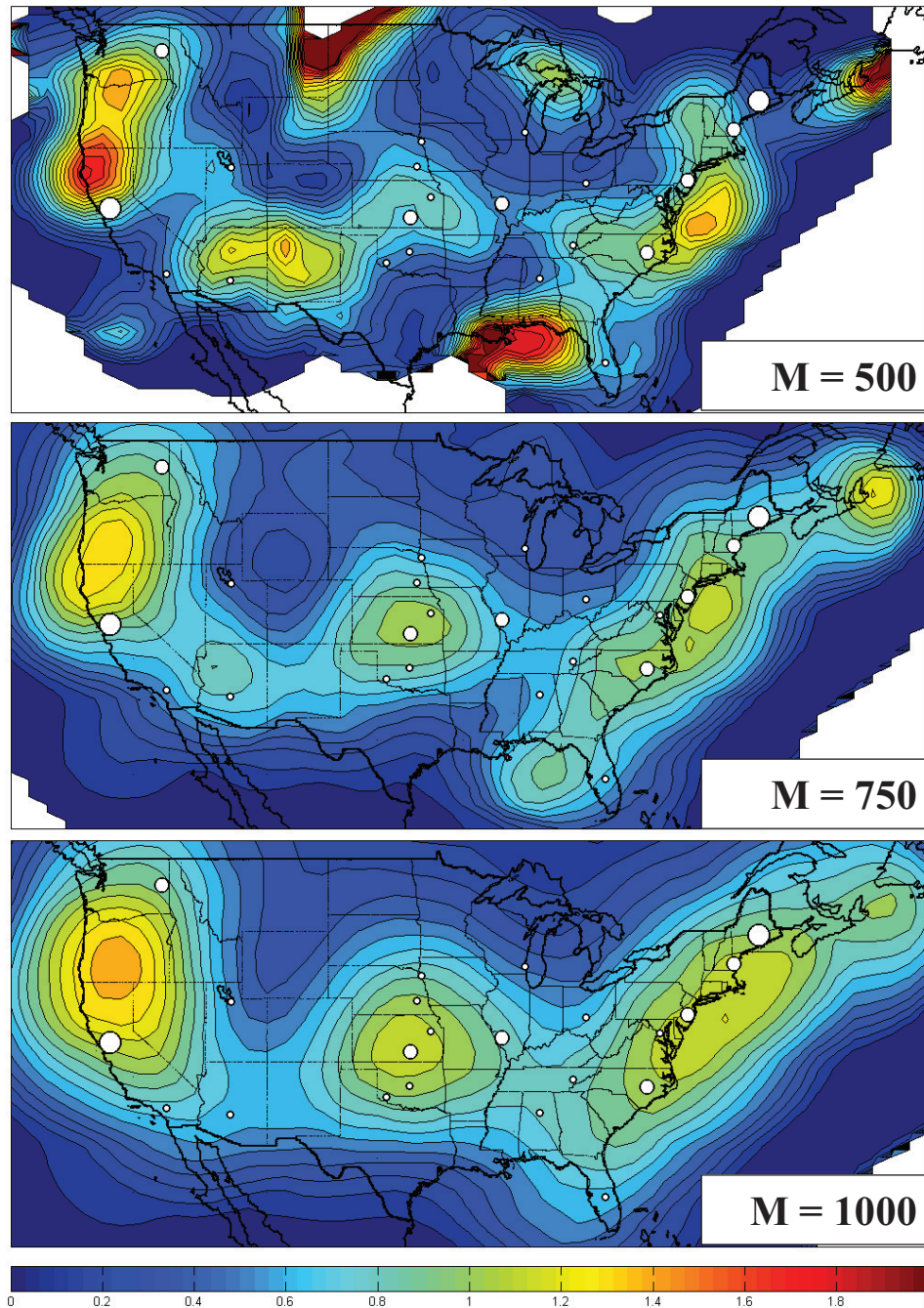


Figure 3.6: TBDMI₁ Maps Generated by the Opt 0708 Basing Strategy

TBDMI₁ Scores for FY12 Basing

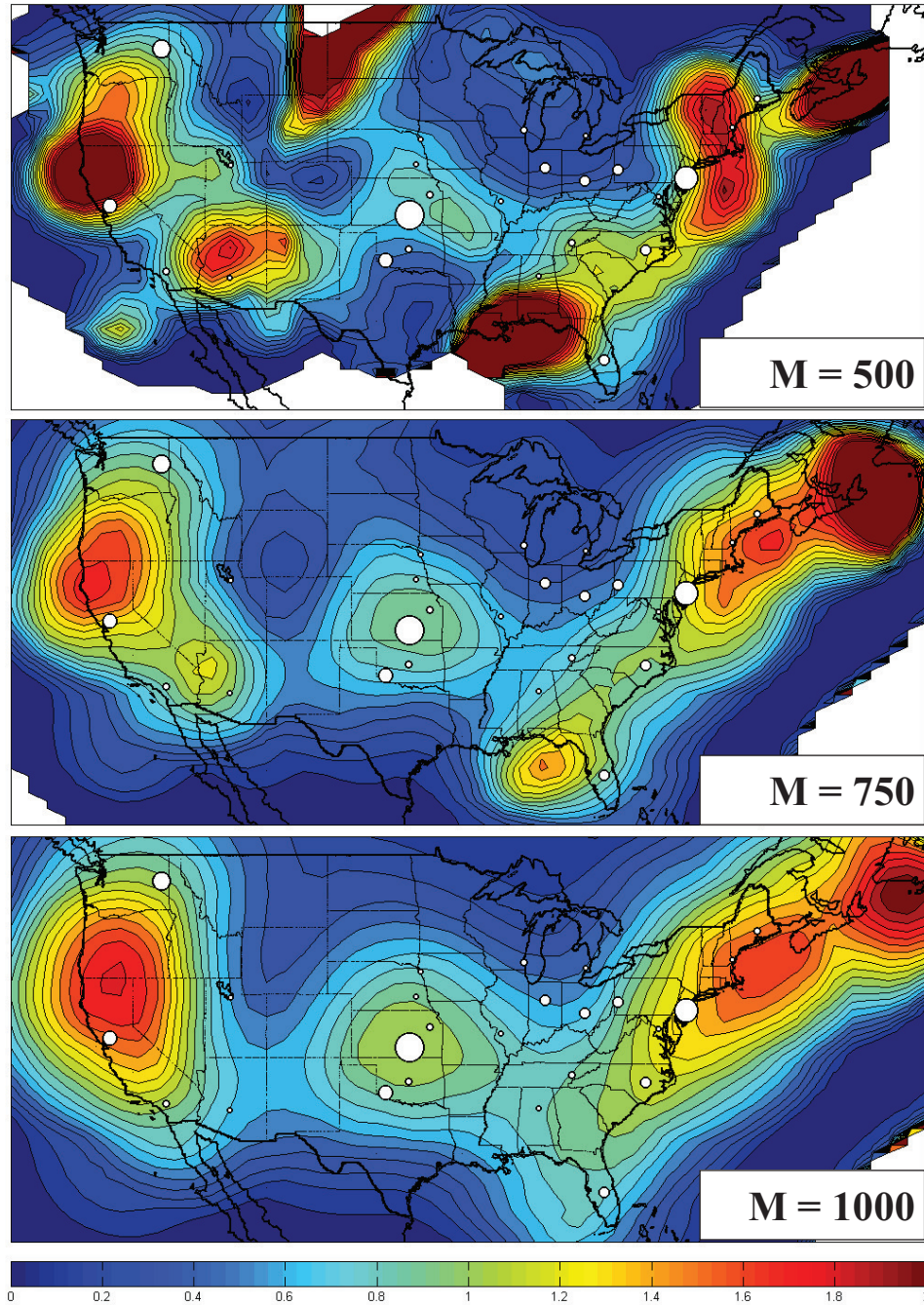


Figure 3.7: TBDMI₁ Maps Generated by the FY12 Basing Strategy

damage is done by reallocating a large number of the tankers currently positioned in Wisconsin, Indiana, and Ohio. Meanwhile the addition of tankers on the west coast has produced a noticeable reduction in the $TBDMI_1$ values in the south west and along the California/Oregon border. Finally increasing the number of tankers along the east coast and distributing tankers more evenly along the east coast appears to have dramatically reduced $TBDMI_1$ values there.

3.4 Comparing Data Sets

Decomposition of AR Demand By Priority

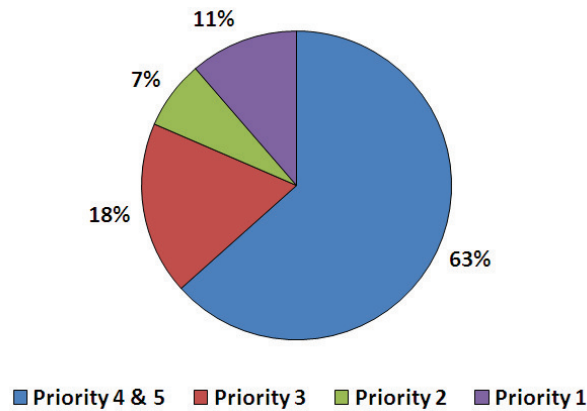


Figure 3.8: Decomposition of demand for AR support by priority level

One of the questions that came up while collecting data and studying results was whether priority 1 and 2 AR events should be included in a strategic basing analysis. Priority 1 and 2 events (hence forth high priority events) are almost certainly related to missions that directly supported the war effort in Iraq or Afghanistan. These events account for less than a quarter of the work done by the tanker fleet but are heavily concentrated along the mid Atlantic coast and out over the north eastern tip of Maine. Consequently, including these events in strategic basing analyses pulls resources towards the east and north east. Priority 3, 4, and 5 events (hence forth low priority events) are mostly related to training and are distributed over the entire Continental United States (CONUS) along with receiver units and practice ranges.

Consequently, in spite of the fact that they represent 81% of the demand for AR support, their importance is diluted.

The argument for leaving high priority events in the analysis is simple and obvious: this is valid data and represents a very important part of the tanker fleet's mission. There are, however, three very good reasons they should not be included. First and foremost is the argument that a long term basing plan, heavily influenced by today's conflicts is not all that strategic. Specifically, if trouble were to suddenly break out in the Pacific, a tanker basing plan sculpted by data from the last 5 years would suddenly look very foolish. In addition to this, there is the argument that dollars and resources will always exist to fly the extra miles to support high priority missions. Meanwhile, dollars for training keep getting cut. In light of that fact, and in anticipation of a time when Iraq and Afghanistan are at peace, it makes a lot of sense to base tankers near the areas in which they are needed to support training efforts. Finally, there is the argument that the data requirements for high priority events far exceed the data requirements of low priority events. Consequently, while it is safe to assume that close to 100% of all high priority events will make it into the data set, it is hard to estimate the comprehensiveness of the the low priority data set. This asymmetry in data capture skews the results even more toward the regions in which high priority events are concentrated and amplifies the wisdom of the previous two arguemnts.

To study the difference made by high priority events, the location routing problem was used to generate an optimal basing strategy for low priority AR events taken from the FY07-FY08 time period. The optimal schedule generated by the fifth basing strategy had an optimal distance value of 28,004,916, which is nearly the same as the FY12 basing plan. The contours of the TBDMI₁ map generated by the fifth basing strategy (figure 3.9) are also very similar to the FY12 basing plan. The main distinctions are in the north east, the south east and the south west. The fifth basing plan has noticeably lower TBDMI₁ scores in the south east and south west, while the FY12 basing plan has noticeably lower TBDMI₁ scores in the north east. Meanwhile, there are only four differences in the way in which the Opt 0708 and the fifth tanker basing plan distributed tankers. Specifically, 36 tankers were removed from Bangor and distributed evenly between Grissom Field (KGUS), Selfridge AFB (KMTC), and McGhee Tyson AFB (KYTS).

TBDMI₁ Scores for Opt 0708 Wo P1 & P2

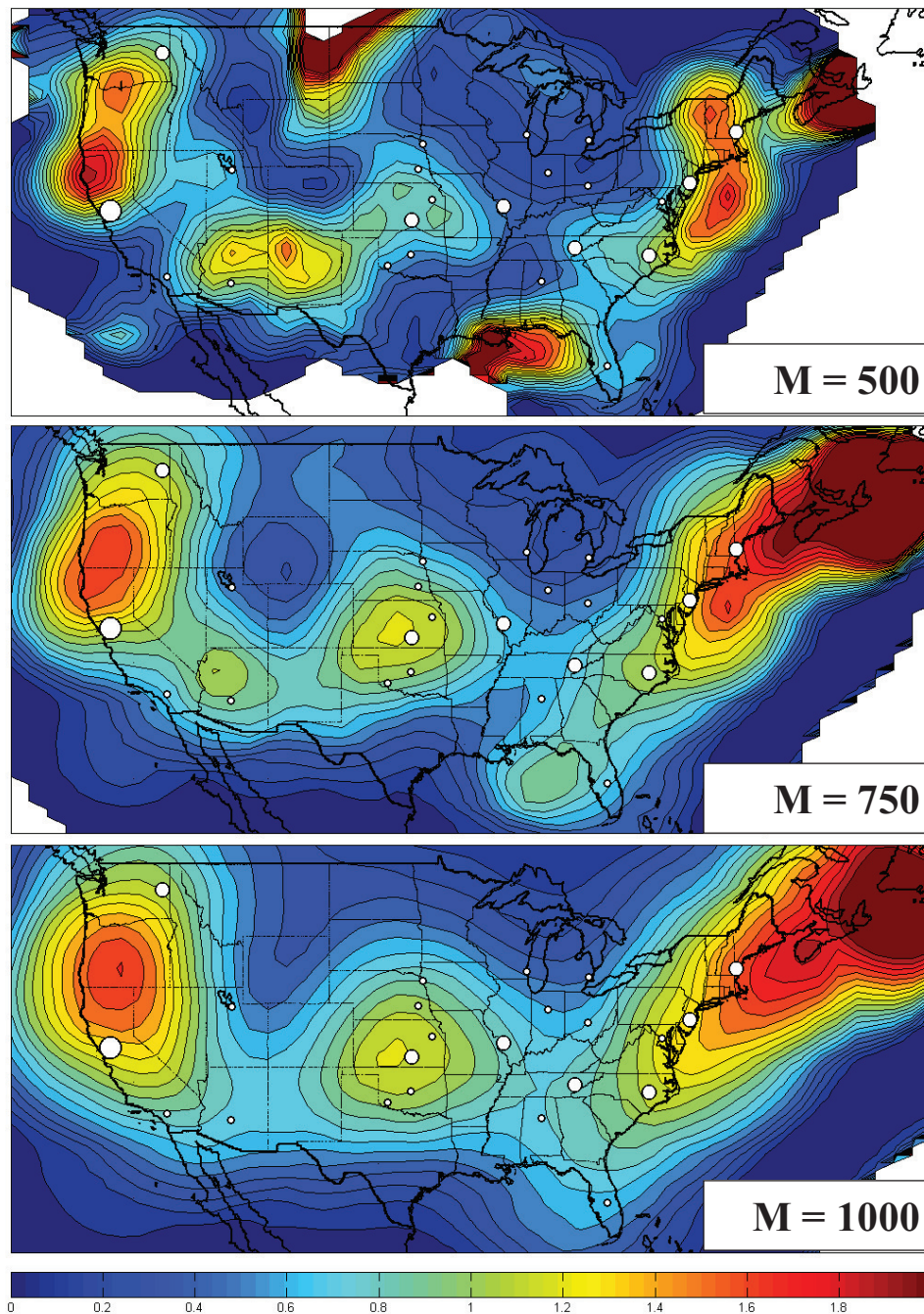


Figure 3.9: TBDMI₁ maps for the fifth basing strategy

TBDMI₁ Scores for Hybrid Strategy

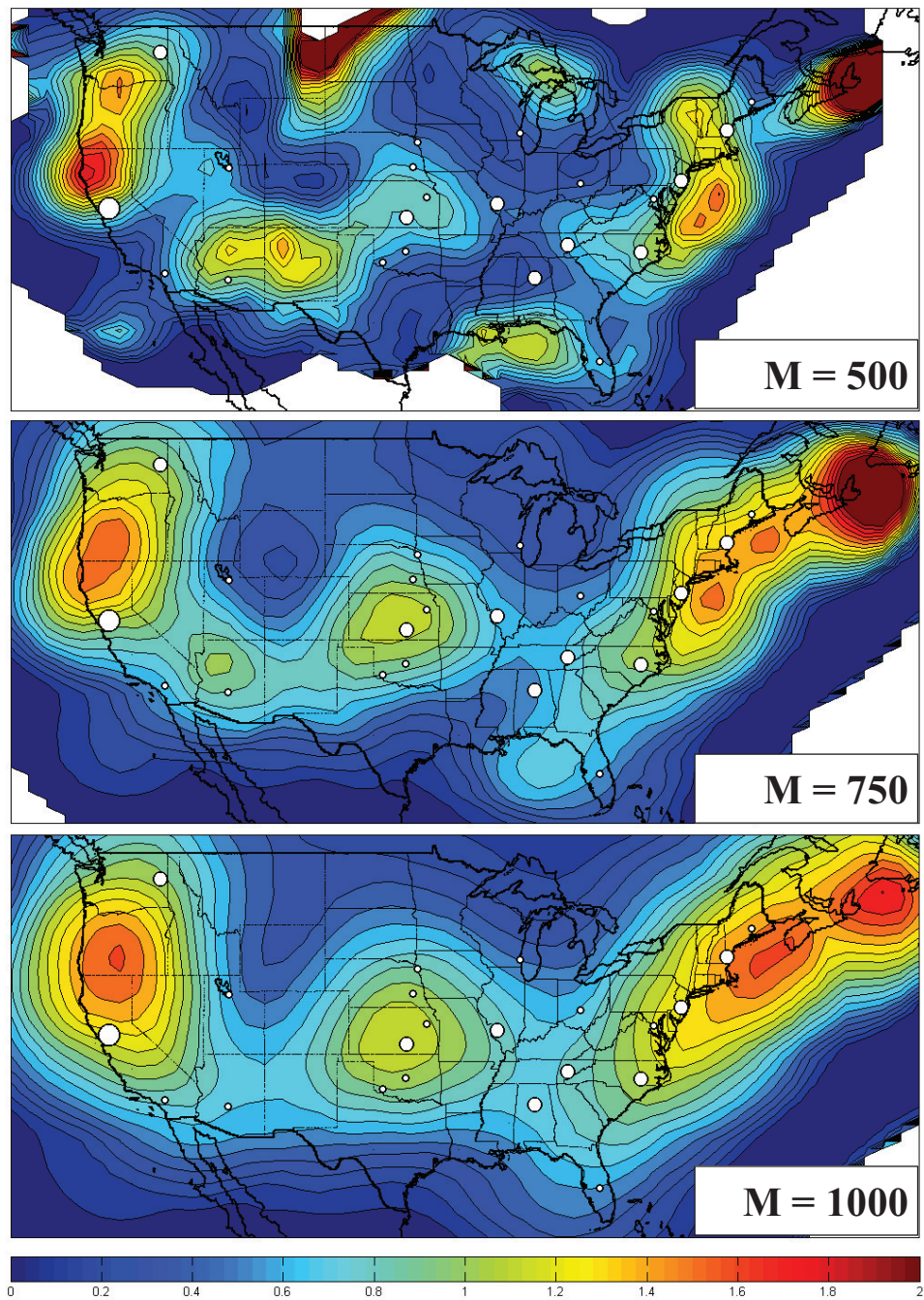


Figure 3.10: TBDMI₁ maps for the sixth basing strategy

Together the previous results and the results from the limited data set suggest a sixth and final basing strategy which acknowledges the increasing importance of the south east (as seen in FY08-FY09 panes of figures 3.3 and 3.4), the ongoing importance of the north east, and serious doubts that tankers are truly needed at Selfridge Air Force Base. This hand made strategy starts with the tanker basing plan generated by the truncated data set, moves the 12 tankers positioned at Selfridge AFB back into Bangor, and moves the 12 tankers positioned at Grissom down to Birmingham. The TBDMI₁ maps produced by the hybrid basing strategy (see figure 3.10) and the previous basing strategies suggest that the region between western Illinois and and Western Pennsylvania can be covered reasonably well by tankers positioned at the corners (e.g. Scott AFB, and Rickenbacker AFB, or Scott AFB and Pittsburgh). It also demonstrates that the south will be well served by an additional 12 tankers somewhere near Birmingham. Finally, considering the fact that the demand in the North East is not 100% permanent, it seems reasonable to expect that surges in AR demand along the north east will be supported by temporarily positioning tankers from other parts of the country at Bangor or Pease.

3.5 Suggestions for Further Research

The location routing model presented in this chapter takes a very simple and narrow view of the the tanker basing problem. Meanwhile, planners have to deal with less tangible factors such as the ability for Air National Guard units to recruit tanker crews and maintenance staff, noise pollution, air space restrictions, and encroachment on surrounding civilian populations. Future research should focus on more detailed models which consider these factors as well as the costs of opening new tanker bases, moving tanker units from their current locations, increasing the capacity of tanker bases, and downsizing or closing existing locations. Also, considering the 10 to 20 year time line involved, realistic models will make an attempt to account for the time value of money.

The time horizon on KC-X basing decisions also makes it critical to develop the ability to accurately forecasts changes in the geographic distribution of AR demand. Currently analysts are forced to assume that the receiver basing structure, practice

range structure, and intensity of receiver activity will stay approximately the same over the course of the next 10 years. This is because a large portion of the AR event records which are readily available to analysts in a query-able form do not reference the receiver unit or the receiver type. As a result it is very difficult to study the structure of current AR demand with respect to the current receiver bed down strategy. By extension, it is very difficult to forecast changes in the geographic distribution of AR demand with changes in the receiver bed down plan.

Finally, because these are rather lofty goals, it might be useful in the near term to consider other narrowly focused tanker basing problems and see how their TBDMI scores stack up to the TBDMI scores of the model presented in this chapter. For example, it may be interesting to study a location routing model which attempts to minimize the maximum distance traveled by any one tanker sortie. It may also be interesting to consider a model which minimizes the number of tanker bases put into service, while satisfying similar scheduling constraints and limiting the maximum round trip distance traveled by a single tanker sortie.

Chapter 4

Optimizing Tanker Training Schedules

4.1 Introduction

Most of the tanker aircraft (e.g. KC-135s) are controlled by individual Air National Guard units, or units in the Air Force Reserves. Because these units cannot be directly tasked by 618 TACC there is little to no central authority coordinating tanker and receiver training schedules. At most, 618 TACC is responsible for managing a web based process called the Horse Blanket and encourages tanker and receiver units to communicate their training requirements and coordinate their schedules through this system. However, because engagement in the Horse Blanket process is optional, a large number of low priority AR training missions are planned over the phone at the unit level. Even when the Horse Blanket is used to schedule AR events, little to no effort is made at the global level to find training schedules which minimize the total distances traveled or maximize the number of receivers supported per mile traveled. In fact most of the AR events supported through the Horse Blanket enter the system already paired to a tanker unit. Thus the system is often prevented from using optimization of any sort to find better schedules.

For the last three years the Air Mobility Command has been looking for ways to improve the situation. The following research was done to provide a first rough estimate on the amount of money that could be saved by reforming the system.

4.2 A Scheduling Model

The Horse Blanket Process is a quarterly process designed to help receiver units and tanker units communicate their training requirements and coordinate a training schedule. In theory, at the beginning of each fiscal quarter, receiver units are suppose to provide the Horse Blanket with a list of their requirements and tanker units are suppose to provide it with their availability. If this was truly the case, the system's optimization tools could be engaged to find an optimal schedule. It is widely believed, however, that receiver units load more requests into the system than they actually need, hoping that enough requests are supported to satisfy their true requirement. Meanwhile it is believed tanker units hold back on posting their availability until they see a receiver request they are willing to support. In addition to this, a large number of events are entered into the system as complete, pre-coordinated, packages.

In spite of the fact that end users don't allow the Horse Blanket process to work as it was designed it is, none the less, a warehouse of primordial scheduling data. Specifically, each AR request entered into the system provides the day, location, start time, and duration of a training event which a receiver unit is willing to support along with the number and type of receiver aircraft the unit is willing to provide. Consequently, a receiver unit's list of requests can be viewed as an accurate calendar of its availability. Meanwhile the list of AR events supported by a tanker unit communicates both the weekly availability of that tanker unit, as well as the mix of receiver types, and number of day and night time events the tanker unit needs in order to satisfy its quarterly training requirements. With this interpretation of the data in mind, consider the optimization problem given by equations (4.1) through (4.10).

$$\min \sum_{i=1}^I \sum_{j=1}^J X_{ij} D_{ij} \quad (4.1)$$

such that:

$$1 \geq \sum_{j=1}^J X_{ij} \quad 1 \leq i \leq I \quad (4.2)$$

$$\text{TWS}_{jh} \geq \sum_{i \in W_h} X_{ij} T_i \quad 1 \leq j \leq J, 1 \leq h \leq H \quad (4.3)$$

$$\text{TNF}_j \leq \sum_{i \in NF} X_{ij} T_i \quad 1 \leq j \leq J \quad (4.4)$$

$$\text{TNH}_j \leq \sum_{i \in NH} X_{ij} T_i \quad 1 \leq j \leq J \quad (4.5)$$

$$\text{TDF}_j \leq \sum_{i \in DF} X_{ij} T_i \quad 1 \leq j \leq J \quad (4.6)$$

$$\text{TDH}_j \leq \sum_{i \in DH} X_{ij} T_i \quad 1 \leq j \leq J \quad (4.7)$$

$$\text{RWDD}_{kh} \leq \sum_{i \in DW_{kh}} X_{ij} R_{ik} \quad 1 \leq k \leq K, 1 \leq h \leq H \quad (4.8)$$

$$\text{RWND}_{kh} \leq \sum_{i \in NW_{kh}} X_{ij} R_{ik} \quad 1 \leq k \leq K, 1 \leq h \leq H \quad (4.9)$$

$$X_{ij} \quad \text{Binary} \quad (4.10)$$

The indices h , i , j , and k refer to week, AR event, tanker unit, and receiver unit IDs respectively. The binary decision variable X_{ij} is equal to 1 if event i is assigned to tanker unit j , and 0 otherwise.

The constraints defined in equation (4.2) require that each AR event is assigned to at most one tanker unit.

The constraints defined by equation (4.3) use the constants TWS_{jh} (Tanker Unit Weekly Supply) and the constant T_i (Number of Tankers Required By Event) to control the number of tanker sorties each tanker unit is expected to generate during each week of the quarter. Note that the sums in these constraints are restricted to the AR events which are scheduled to occur during a given week ($i \in W_h$). Also note that this constraint, and the ones that follow, tacitly assume that each tanker sortie only supports one AR event.

The constants TNF_j (Tanker Unit Night Fighter Requirement), TNH_j (Tanker Unit Night Heavy Requirement), TDF_j (Tanker Unit Day Fighter Requirement) and TDH_j (Tanker Unit Day Heavy Requirement) are used with T_i in constraints (4.4) through

(4.7) to ensure that each tanker unit gets the number of day and night time sorties it needs over the quarter and to maintain each unit's mix of receiver aircraft. Note that the sums in these constraints are restricted to AR events which are associated with night fighters ($i \in \text{NF}$), night heavies ($i \in \text{NH}$), day fighters ($i \in \text{DF}$), and day heavies ($i \in \text{DH}$), respectively.

The constants RWDD_{kh} (Receiver Unit Weekly Day Time Demand) RWND_{kh} (Receiver Unit Weekly Night Time Demand) are used along with the constant R_i (the number of receiver aircraft participating in an event) in constraints (4.8) and (4.9) to guarantee that each receiver unit is provided a minimum level of day and night time support in every week of the quarter. Note that the sums in these constraints are restricted to day or night time events of a particular receiver unit and week ($i \in \text{DW}_{kh}$ and $i \in \text{NW}_{kh}$, respectively).

Finally, the objective function of this problem uses the distance D_{ij} between the i^{th} AR event and j^{th} tanker unit to compute the total distance flown between the tanker units, and the supported AR events. Minimizing this objective should drive the model toward the schedule which provides receiver units the same minimum level of weekly support while maintaining both the weekly operations tempo and receiver portfolios of each tanker unit.

4.3 Results

The optimization model given in equations (4.1) through (4.10) was used to evaluate the Horse Blanket data of each quarter from FY07-2 through FY10-3. It was found that reforming the Horse Blanket System or its practice of use could reduce the average number of miles flown per quarter by as much as 23%. Assuming average ground speeds of 420 miles per hour, and average tanker operating costs of \$7,000 per hour [4] this amounts to average quarterly savings of \$7,424,039. Over the three complete years of data, this translates to an average annual savings of \$26,454,956. While the real savings from reform will be less than the amounts suggested by this study, it is unlikely that they will be an order of magnitude less. Finally, these results were recently used in presentations that convinced senior leaders at HQ AMC to engage the human resources needed to reform the Horse Blanket process.

QRTR	MILES			Dollars			% DIFF
	HB MILES	OPT MILES	ABS DIFF	HB COST	OPT COST	ABS DIFF	
FY07-2	2,390,246	1,831,517	558,729	39,837,433	30,525,283	9,312,150	23.38%
FY07-3	2,636,532	1,720,960	915,572	43,942,200	28,682,667	15,259,533	34.73%
FY07-4	2,297,852	1,707,484	590,368	38,297,533	28,458,067	9,839,467	25.69%
FY08-1	2,001,947	1,425,710	576,237	33,365,783	23,761,833	9,603,950	28.78%
FY08-2	1,928,148	1,469,946	458,202	32,135,800	24,499,100	7,636,700	23.76%
FY08-3	2,041,412	1,548,616	492,796	34,023,533	25,810,267	8,213,267	24.14%
FY08-4	1,652,343	1,324,980	327,363	27,539,050	22,083,000	5,456,050	19.81%
FY09-1	1,360,870	1,042,903	317,967	22,681,167	17,381,717	5,299,450	23.36%
FY09-2	1,522,343	1,222,715	299,628	25,372,383	20,378,583	4,993,800	19.68%
FY09-3	1,471,713	1,173,874	297,839	24,528,550	19,564,567	4,963,983	20.24%
FY09-4	2,207,274	1,721,781	485,493	36,787,900	28,696,350	8,091,550	22.00%
FY10-1	1,714,507	1,420,320	294,187	28,575,117	23,672,000	4,903,117	17.16%
FY10-2	1,426,747	1,140,058	286,689	23,779,117	19,000,967	4,778,150	20.09%
FY10-3	1,993,610	1,658,487	335,123	33,226,833	27,641,450	5,585,383	16.81%
TOTALS	26,645,544	20,409,351	6,236,193	444,092,400	340,155,850	103,936,550	23.98%

AVERAGE QRTLTY Savings \$ 7,424,039

Figure 4.1: Potential quarterly savings

QRTR	MILES			Dollars			% DIFF
	HB MILES	OPT MILES	ABS DIFF	HB COST	OPT COST	ABS DIFF	
FY07-4 to FY08-3	8,269,359	6,151,756	2,117,603	137,822,650	102,529,267	35,293,383	25.61%
FY08-4 to FY09-3	6,007,269	4,764,472	1,242,797	100,121,150	79,407,867	20,713,283	20.69%
FY09-4 to FY10-3	7,342,138	5,940,646	1,401,492	122,368,967	99,010,767	23,358,200	19.09%
3 Yr Total	21,618,766	16,856,874	4,761,892	360,312,767	280,947,900	79,364,867	22.03%

AVG Annual Savings \$ 26,454,956

Figure 4.2: Potential annual savings

4.4 Directions of Future Research

There are three areas of research needed to help AMC reform the Horse Blanket Process. First, planners would like to know when it is advantageous to temporarily reposition tankers near an area with a local surge in AR activity. To do this correctly they will also need to know how to identify the resources that will be repositioned. Second, data support the assertion that 90% of all round robin tanker sorties which support an AR event only support one AR event. As a result, additional savings could be realized if a larger share of tanker sorties supported 2 or more AR events. Thus it will soon be necessary to formulate AR event scheduling as a Vehicle Routing Problem with time windows. Finally in order for a more centralized scheduling process to work and maintain the trust and respect of its end users, it will need to be able to handle last minute requests, weather dealys, and maintenance cancellations without completely falling apart. Further research into the details of these events, and scheduling in the face of uncertainty will be necessary to handle this challenge.

References

- [1] Martha L. Abell and James P. Braselton. *Modern Differential Equations*. Thomas Learning, Toronto, Ontario, second edition, 2001.
- [2] Dimitri P. Bertsekas. *Nonlinear Programming*. Athena Scientific, Belmont, MA, second edition, 1999.
- [3] Todd E. Combs. *A Combined Adaptive Tabu Search and Set Partitioning Approach for the Crew Scheduling Problem with an Air Tanker Crew Application*. PhD thesis, Air Force Institute of Technology, 2002.
- [4] Bradford Davis. Interviews, correspondences, and answers to random questions. Deputy Chief Current Operations Branch HQ AMC A3OO USAF, 2008 - 2010.
- [5] LtCol Lee Erickson. Interviews, correspondences, and answers to random questions. Chief Installations Branch HQ AMC A8PI USAF, 2009-2010.
- [6] Francis J. Hale. *Introduction to Aircraft Performance Selection, and Design*. John Wiley and Sons, New York, NY, 1984.
- [7] Frederick S. Hillier and Gerald J. Lieberman. *Introduction to Operations Research*. McGraw-Hill, Inc, St. Louis, Mo, sixth edition, 1995.
- [8] Matthew R. Jardin and Arthur E. Bryson Jr. Neighboring optimal aircraft guidance in winds. *Journal of Guidance, Control, and Dynamics*, 24(4):710–715, July-August 2001.
- [9] Robert E. Burks Jr. *An Adaptive Tabu Search Heuristic For the Location Routing Pickup and Delivery Problem With Time Windows with a Theater Distribution Application*. PhD thesis, Air Force Institute of Technology, 2006.
- [10] C. Edward Lan and Jan Roskam. *Airplane Aerodynamics and Performance*. Roskam Aviation and Engineering Corporation, Ottawa, Kansas, 1980.
- [11] Mark J. MacDonald. Handbook for tanker employment modeling. Master’s thesis, Air Force Institute of Technology, 2005.
- [12] Jeffrey R. Miller. A capacitated facility location approach for the tanker employment problem. Master’s thesis, Air Force Institute of Technology, 2005.

- [13] Richard E. Rosenthal. *GAMS - A User's Guide*. GAMS Development Corporation, Washington, DC, 2008.
- [14] Bryan Russina and Brady Ruthsatz. The quick look tool for tanker deployment. Master's thesis, Center for Optimization and Semantic Control Washington University, St. Louis Missouri, 1999.
- [15] Peter F. Szabo. Interviews, correspondences, and answers to random questions. Chief Analysis Assessments Division HQ AMC A9A USAF, 2005 - 2010.
- [16] Paolo Toth and Daniele Vigo. *The Vehicle Routing Problem*. Society for Industrial and Applied Mathematics, Philadelphia, PA, 2002.
- [17] Victor Duane Wiley. *The Aerial Fleet Refueling Problem*. PhD thesis, The University of Texas At Austin, 2001.
- [18] Lee Winter. Interviews, correspondences, and answers to random questions. Contractor 618 TACC, 2008 - 2010.
- [19] Abdulrahman Yamani, Thom J. Hodgson, and Louis A. Martin-Vega. Single aircraft mid-air refueling using spherical distances. *Operations Research*, 38(5):792–800, September-October 1990.
- [20] Kirk Yost. A note on computing tanker fuel burn. An unpublished internal memo.

Vita

Allen B. McCoy III

Date of Birth February 9, 1977

Place of Birth Saint Louis, Missouri

Degrees B.S. Economics & Mathematics, May 1999
 M.S. Systems Science & Mathematics, May 2008
 D.Sc. Systems Science & Mathematics, May 2010

May 2010

Modeling Aerial Refueling Operations, McCoy, D.Sc. 2010